

1 New probabilistic price forecasting models: Application to the Iberian Electricity

2 Market

3 Claudio Monteiro^a, Ignacio J. Ramirez-Rosado^b, L. Alfredo Fernandez-Jimenez^{c*}, Miguel Ribeiro^a

4 ^aFEUP, Faculdade Engenharia Universidade do Porto, Porto, Portugal

5 ^bElectrical Engineering Department, University of Zaragoza, Zaragoza, Spain

6 ^cElectrical Engineering Department, University of La Rioja, Logroño, Spain

7 Abstract

8
9
10 This article presents original Probabilistic Price Forecasting Models, for day-ahead hourly price
11 forecasts in electricity markets, based on a Nadaraya–Watson Kernel Density Estimator approach. A
12 Gaussian Kernel Density Estimator function is used for each input variable, which allows to calculate
13 the parameters of the probability density function (PDF) of a Beta distribution for the hourly price
14 variable. Thus, valuable information is obtained from PDFs such as point forecasts, variance values,
15 quantiles, probabilities of prices, and time series representations of forecast uncertainty. A Reliability
16 Indicator is also introduced to give a measure of “reliability” of forecasts. The Probabilistic Price
17 Forecasting Models were satisfactorily applied to the real-world case study of the Iberian Electricity
18 Market. Input variables of these models include recent prices, power demands and power generations
19 in the previous day, power demands in the previous week, forecasts of demand, wind power generation
20 and weather for the day-ahead, and chronological data. The best model, corresponding to the best
21 combination of input variables that achieves the lowest MAE, obtains one of the highest Reliability
22 Indicator values. A systematic analysis of MAE values of the Probabilistic Price Forecasting Models
23 for different combinations of input variables showed that as more types of input variables were
24 considered in these models, MAE values improved and Reliability Indicator values usually increased.

25
26 **Keywords:** short-term forecasting; market prices; Iberian electricity market; electricity prices;
27 probabilistic forecast

28 Nomenclature

29		47	GFS	Global Forecast System
30		48		
31	<i>Abbreviations</i>	49	<i>Variables</i>	
32		50		
33	PPFM	51	x	explanatory price variable
34	DAEPF	52	y	electricity price variable
35	NW-KDE	53	$x_{v,new}$	explanatory price variable for dimension v for future hour (<i>new</i>)
36		54		
37	PDF	55	$x_{v,p}$	explanatory price variable for dimension v for past instant p
38	MAE	56		
39	RI	57	$\{x_{1,new}, \dots, x_{v,new}, \dots, x_{m,new}\}$	generic case
40	SVM	58		for future hour (<i>new</i>)
41	MIBEL	59	x_{new}	explanatory price variable for future hour (<i>new</i>)
42	OMIE	60		
43	TSO	61	x_v	explanatory price variable for dimension v
44	REE	62		
45	REN	63	y_{new}	electricity price variable for future hour (<i>new</i>)
46	NWP	64		

65	y'_{new}	standardized electricity price variable	116	$F_{new}(\alpha_{new}, \beta_{new}, y_{new,min}, y_{new,max})$	Beta cumulative
66		between 0 and 1 corresponding to y_{new}	117		distribution function for future hour (new)
67	y_p	electricity price variable for instant p	118	$f(y'_{new}; \alpha_{new}, \beta_{new})$	PDF of a Beta distribution, in $[0 ; 1]$,
68	y'_p	standardized variable between 0 and 1	119		for y'_{new}
69		corresponding to y_p	120	$f_{new}(y_{new}; \alpha_{new}, \beta_{new}, y_{new,min}; y_{new,max})$	PDF of a
70			121		Beta distribution for future hour (new)
71	<i>Elements</i>		122	$F_{new_q}(y_q; \alpha_{new_q}, \beta_{new_q}, y_{new_q,min}, y_{new_q,max})$	Beta
72			123		cumulative distribution function for new
73	$[Y_{new}]$	element associated with y_{new}	124		case q for future hour (new)
74	$[Y'_{new}]$	element associated with y'_{new}	125		
75	$[X_{new}]$	set of elements associated with explanatory	126	<i>Frequencies</i>	
76		variables $x_{v,new}$.	127		
77			128	$f_{obs,i}$	observed frequencies in the interval i
78	<i>Numerical values</i>		129	$f_{tar,i}$	target frequency in the interval i
79			130		
80	n	number of cases of the historical dataset	131		<i>Data for application of PPFM models to MIBEL</i>
81	m	number of price explanatory variables	132		
82	$x_{new,max}$	highest limit value for x_{new}	133	$p_{D-6,h}$	price for hour h of day $D-6$
83	$x_{new,min}$	lowest limit value for x_{new}	134	$p_{D,h}$	price for hour h of the day D
84	$x_{v,max}$	maximum value of x_v of the historical	135	w_{D+1}	week
85		dataset of cases	136	$\hat{T}_{D+1,h D,t}$	regional weighted forecasted hourly
86	$x_{v,min}$	minimum value of x_v of the historical dataset	137		temperature for hour h of day $D+1$, obtained
87		of cases	138		at hour t of the day D
88	$y_{new,max}$	the highest limit value for y_{new}	139	$\hat{I}_{D+1,h D,t}$	regional weighted forecasted hourly
89	$y_{new,min}$	the lowest limit value for y_{new}	140		irradiations for hour h of day $D+1$, obtained
90	$n-new,min$	number related to $y_{new,min}$	141		at hour t of the day D
91	$n-new,max$	number related to $y_{new,max}$	142	$\hat{v}_{D+1,h D,t}$	regional weighted forecasted hourly wind
92	bl_a	basic level of activation	143		speeds for hour h of day $D+1$, obtained at
93	$bl_{a,std}$	standardized basic level of activation	144		hour t of the day D
94	F_{chg}	factor between 0 and 1	145	$HG_{D-1,h}$	hydropower generation for hour h of day $D-$
95	N_p	minimum number of activated points from	146		1
96		the historical dataset	147	$SG_{D-1,h}$	solar power generation and power
97	NQ	total number intervals	148		cogeneration for hour h of day $D-1$
98	N	number of elements in the out-sample	149	$CG_{D-1,h}$	coal power generation for hour h of day $D-1$
99		dataset	150	$CCG_{D-1,h}$	combined cycle power generation for hour h
100			151		of day $D-1$
101	<i>Parameters</i>		152	$WG_{D-1,h}$	wind power generation hour h of day $D-1$
102			153	$NG_{D-1,h}$	nuclear power generation hour h of day $D-$
103	h_v	bandwidth for dimension v	154		1
104	α_{new}	parameter α of PDF of a Beta distribution	155	$LD_{D-1,h}$	power demand hour h of day $D-1$
105		for future hour (new)	156	$LD_{D-6,h}$	power demand hour h of day $D-6$
106	β_{new}	parameter β of PDF of a Beta distribution for	157	$\hat{W}G_{D+1,h D,t}$	wind power generation forecast for hour h of
107		future hour (new)	158		day $D+1$, obtained at hour t of the day D
108	$(\alpha_{new}, \beta_{new}, y_{new,min}, y_{new,max})$	parameters of a PDF	159	$\hat{L}D_{D+1,h D,t}$	power demand forecast for hour h of day
109		of a Beta distribution for future hour (new)	160		$D+1$, obtained at hour t of the day D
110	$(\alpha_{new_q}, \beta_{new_q}, y_{new_q,min}, y_{new_q,max})$	parameters of a PDF	161	P_{real_T}	real hourly price value for the hour T
111		of a Beta distribution for new case q	162		
112			163		
113	<i>Functions</i>		164		<i>Forecasts from the application of PPFM models to</i>
114			165		<i>MIBEL</i>
115	$K_v(x_{v,p}; x_{v,new}, h_v)$	kernel density estimation function			

166		169	$P_{forecast_T}$	expected value of hourly price of a PPMF
167	$\hat{p}_{D+1,h D,t}^d$	170		model for the hour T .
168		171		

172

173

174

175

176 **1. Introduction**

177

178 1.1. *Context of this research related to the day-ahead electricity price forecasting*

179

180 In the last 25 years the transition from monopolistic power sectors to competitive ones has led
 181 to the trade of electricity under market rules. In the market paradigm, the economic operation of the
 182 power system is based on price signals that are holistically influenced by all the market agents, which
 183 try to achieve their economic interests. These price signals are mainly generated in the day-ahead
 184 market, which influences all the remaining market prices (e.g., intraday markets, derivative product
 185 markets, and bilateral markets). Knowing in advance the prices that will be settled by the day-ahead
 186 electricity market is essential for the price-makers' agents, guiding the bidding decision-making
 187 process in order to maximize their economic profit.

188

189 Furthermore, knowing the prices in advance is even important for the least relevant agents
 190 (those who, due to their low volume of trading operations, do not influence the price value), who can
 191 evaluate the risk of anomalous prices in advance and, consequently, respond to high or low price
 192 forecasts by managing their electricity consumption and/or their self-power generation.

193

194 Therefore, a significant effort has been made in recent years to develop Day-Ahead Electricity
 195 Price Forecasting models (DAEPF models). Most of the published DAEPF models are focused on
 196 point (spot) forecasts, that is, they provide the values of forecasted hourly electricity prices without
 197 any additional information. However, these DAEPF models that only give point forecasts can be
 198 inadequate for trading purposes because they do not show the uncertainty associated with the price
 199 forecasts, which is essential for risk-based market decisions. Point (spot) forecasts do not offer
 200 information to support trading associated with market risks. Market decisions based on point forecasts
 201 are suitable when the economic impact of the deviation (between forecast value and real value) is
 202 linearly dependent on the absolute value of the deviation. However, probabilistic price forecasting
 203 models are able to provide information regarding the uncertainty of the price forecasts. They have
 204 become essential models for making proper risk-based decisions when the magnitude of the price (or
 205 magnitude of the deviation) has a higher relative impact on more extreme price values, that is, when it
 206 is imperative to know the probability of occurrence of the different level of prices (or magnitude of
 207 deviations).

208

209 1.2. *Literature review*

210

211 DAEPF models centered on point (spot) forecasts are essentially based on classic time series
212 models or computational intelligence models, although some models combine both approaches.
213 Classic time series DAEPF models described in the literature use a wide variety of techniques [1].
214 Some works describe the application of only one technique [2], while others apply a set of techniques
215 for developing several models and comparing their forecasting results. The techniques used include
216 exponential smoothing [3], multiple regression [4, 5], time-varying regression [6, 7], Box-Jenkins and
217 derived models [8-10], econometric models [11] and GARCH (Generalized Auto-Regressive
218 Conditional Heteroskedasticity) [12, 13]. Usually, the simpler techniques are used to develop
219 benchmark models for comparison purposes [14]. Computational intelligence DAEPF models are
220 based principally on artificial neural networks [15-17], fuzzy systems [18, 19], and support vector
221 machines (SVM) [20, 21]. Some of both families of DAEPF models need explanatory variables such
222 as load demand, meteorological variables (mainly temperature), and wind or solar electric power
223 production, the values of which, for the forecasting horizon, are obtained by means of other short-term
224 forecasting models [22, 23]. Preprocessing techniques such as wavelet decomposition have been used
225 to improve model performance [24], optimization methods have been used to tune the structure of the
226 DAEPF model [25-27], or classifiers have been used as an additional module to forecast price spikes
227 [28]. Combinations of forecasts from different DAEPF models have been studied, and reveal a more
228 accurate and robust point forecast [5, 29]. Similar approaches, using advanced forecasting techniques,
229 have been also applied in other electric energy sectors, such as load forecasting [30], wind power
230 forecasting [31], solar power forecasting [32], or building energy demand forecasting [33].

231
232 Electricity market agents can need price forecasts for risk-based decisions in diverse situations.
233 They can use probabilistic price forecasts for risk-based decisions by pondering the risk based on
234 probability measures. The impact of these decisions can depend on the probability of having prices
235 higher/lower than a threshold value. In this sense, probabilistic price forecasting models have an
236 important added value compared with non-probabilistic price forecasting models. Probabilistic models
237 also overcome the limitations of spot forecasts by allowing the generation of scenarios for the day-
238 ahead for several kinds of power-producers [34-38]. Some kinds of DAEPF probabilistic models have
239 been identified in the literature [1] according to their output values: interval forecasts (or also known
240 as prediction intervals), density forecasts, and threshold forecasts, although this last kind can be
241 considered as a special instance of prediction intervals.

242
243 Most of the early works describing DAEPF probabilistic models focused on prediction
244 intervals, since estimating these can help utilities and independent power producers to submit effective
245 bids with low risks [38]. The techniques utilized include support vector machines with heteroscedastic
246 variance equation and the maximum likelihood estimation [39], an extreme learning machine with
247 bootstrapping method [23] or with an estimation of the noise variance [40], delta and bootstrap
248 methods [41], a recursive dynamic factor analysis [42], the variational heteroscedastic Gaussian
249 process [43], and quantile regression averaging with principal component analysis [44]. The main
250 application of threshold forecasting is related to demand-side management, where several data-mining
251 techniques used as classifiers have been used [45, 46]. In spite of everything, interval and threshold

252 forecasts only allow decisions related to the corresponding specific intervals or thresholds. However,
253 density forecast, which is the subject of the probabilistic price forecasting models presented in this
254 article, provides suitable probabilistic information for any risk-based decision usage.

255

256 A much better approach to building DAEPF probabilistic models is the forecasting of the
257 probability density function (PDF) or density forecasting. In any field of application, a density forecast
258 of a random variable at some future time is an estimate of the probability distribution of the possible
259 future values of that variable. On one hand, it gives a complete description of the uncertainty associated
260 with a prediction and overcomes the main deficiency of a point forecast (from non-probabilistic
261 models), which does not provide any information about the associated uncertainty [47]. On the other
262 hand, obtaining an entire forecast density provides more complete information than single prediction
263 intervals. However, there are only a few works that deal with the development of short-term
264 probabilistic forecasting models based on PDFs for electric energy applications, such as load
265 forecasting [48, 49], solar power forecasting [50, 51], wind power forecasting [52, 53], or electricity
266 price forecasting [54, 55].

267

268 Thus, the most interesting DAEPF probabilistic models (i.e., probabilistic price forecasting
269 models for probabilistic forecasts of the day-ahead hourly price) are focused on probability density
270 functions (PDFs); however there is a scarcity of probabilistic price forecasting models based on them.
271 In the case of electricity price density forecast, Serinaldi [54] proposes the use of the Generalized
272 Additive Models for Location, Scale, and Shape (GAMLSS) [56] to obtain the entire day-ahead
273 electricity price distribution function; the explanatory variables used by the forecasting model are past
274 prices, electricity loads (including the day-ahead forecasts, if available) and chronological information.
275 Another approach is the one proposed by Jónsson *et al.* [55], where the densities for the day-ahead
276 electricity prices are obtained using a time-adaptive quantile regression model and the approximation
277 of the distribution tails. The forecasting model uses as input variables forecasts of spot electricity prices
278 (provided by a spot DAEPF model), forecasts of system load and forecasts of wind power production.

279

280 *1.3. Objectives and characteristics of the models of this research and their application*

281

282

283 This article describes original Probabilistic Price Forecasting Models (PPFM models) for
284 probabilistic forecasts of the day-ahead hourly price in electricity markets focused on probability
285 density functions (PDFs) of Beta distributions. Main novel characteristics of PPFM models and their
286 application are outlined in the following paragraphs.

287

288 The PPFM models provide parametric probabilistic forecasts, represented by the PDF of a Beta
289 distribution, for each hour of the forecast price (output variable). This parametric approach of the
290 output variable provides significant advantages because it gives full information about the uncertainty
291 of price forecasts useful for downstream risk-based decision-making tools.

292

293 The extensive set of input variables of the PPFM models consists of large historic time series
294 of hourly prices in previous days, regional-aggregated hourly power generations (hydropower
295 generation, wind power generation, solar power generation and power cogeneration, nuclear power
296 generation, combined cycle power generation and coal power generation), and hourly power demand
297 in the previous day and in the previous week. Furthermore, this set of input variables also includes
298 hourly time series records of forecasts of regional-aggregated hourly power demands, forecasts of wind
299 power generation and forecasts of weather (hourly wind speed, temperature, and irradiation) in the
300 region for the day-ahead as well as chronological data. The intrinsic uncertainties associated with price
301 forecasts are influenced by these different kinds of explanatory price variables (input variables). These
302 variables affect the expected value of price, as well as the price forecast uncertainty.

303
304 The new PPFM models are based on a Nadaraya–Watson Kernel Density Estimator (NW-
305 KDE) approach [57, 58] using a suitable Gaussian KDE function for each one of its input variables,
306 i.e. explanatory price variables. The NW-KDE approach applied to historical cases (historical data of
307 explanatory price variables and the hourly price historical data), directly obtains the corresponding
308 expected and variance values. They allow us to calculate, in a straightforward way, the essential
309 parameters of the probability density function (PDF) of a Beta distribution that describes the behavior
310 of the price variable for each forecasting hour. Then, this PDF function allows the expected value of
311 the hourly price variable to be determined (i.e. point forecast of hourly price) as well as a variety of
312 useful quantitative probabilistic results of the probabilistic forecast of each PPFM model. These
313 parametric representations (of PDFs) by Beta distributions are advantageous (for downstream usage
314 of the forecast uncertainty) when compared with other approaches.

315
316 A new Reliability Indicator (*RI*) is introduced to assess the uncertainty associated with
317 probabilistic price forecasts; the *RI* gives a quantitative measure (from 0% to 100%) of “reliability” of
318 forecasts of PPFM models. This article also presents a novel representation of “reliability diagram”,
319 associated with the *RI*, which allows the evaluation of the performance of the PDF of Beta distributions
320 to be carried out. “Forecast cases” that fall outside the limits of the PDF are identified by such suitable
321 “reliability diagram”.

322
323 The *RI* values for PPFM models in the real-life case study are also included in this article. Then,
324 a comparison of the PPFM model’s performances revealed that *RI* (“reliability”) values usually
325 improved, and that MAE error values improved when more input variable types (chronological
326 variables, price variables, power demand variables, weather forecast variables, and power generation
327 variables) were considered in the PPFM models.

328
329 An original procedure is used to calibrate the bandwidths of the kernel Gaussian functions
330 involved in the NW-KDE approach. This procedure uses an iterative process to seek successive
331 bandwidth values, for each explanatory variable, which in turn achieve a near optimal *RI* value for
332 each “forecast case” (“new case”).

333

334 The real-life case study of the Iberian Electricity Market (MIBEL) was used to satisfactorily
335 test the PPFM models. As far as we know, this is the first time that probabilistic price forecasting
336 models, based on the NW-KDE approach, have successfully been applied to the Iberian Electricity
337 Market. In this article, firstly, suitable studies of input variable selection for PPFM models led to the
338 determination of reasonable combinations of variables (grouped by their common characteristics). The
339 selection process allowed us to carry out a systematic analysis of Mean Absolute Error (MAE) values
340 of PPFM models in the real-life case study, in order to find the best input variable combination
341 associated with the lowest MAE value, that is, to find the best PPFM model. Furthermore, these studies
342 could determine the relative importance of each input variable. Secondly, a description of the main
343 results of forecast examples of this best PPFM model is included in terms of hourly probability density
344 functions of Beta distributions for hourly price forecasts, time series representations of price forecast
345 uncertainty, expected and variance values of hourly price, and other valuable probabilistic information.
346 Examples of other valuable information are quantiles and probabilities relative to given values of the
347 price (probabilities of prices exceeding or failing to exceed a threshold value). This information can
348 be used to assess the risk in trading operations in electricity markets.

349

350 *1.4. Contributions of this research*

351

352 From the above sub-sections in this Introduction, the novelty and contributions of this article
353 are summarized as follows:

354

- 355 • New PPFM models based on NW-KDE using Gaussian KDE functions for their input price
356 explanatory variables.
- 357 • Very extensive set of input variables of PPFM models consisting of large time series of hourly
358 historical values of price, power generations, demands, and forecasted values of demands, wind
359 speeds, temperatures, and irradiations, as well as chronological data.
- 360 • Probability density functions of Beta distributions for the hourly prices of each PPFM model.
- 361 • Reliability Indicator (*RI*) to assess the uncertainty associated with probabilistic price forecasts
362 of each PPFM model.
- 363 • Calibration procedure of bandwidths of the Gaussian functions of PPFM models.
- 364 • Straightforward determination of expected values of hourly prices, variance values, quantiles,
365 probabilities of prices exceeding or failing to exceed a threshold value, and time series
366 representations of forecast uncertainty of each PPFM model.
- 367 • Successful application of the new PPFM models to the Iberian Electricity Market (MIBEL).
368 The first time that probabilistic price forecasting models based on NW-KDE are applied to
369 MIBEL.

370

371 The PPFM models, their PDF functions for hourly price forecasts and practical probabilistic
372 information from such PDF functions can be useful for agents of the day-ahead electricity markets and
373 the power industry.

374

375 *1.4. Structure of this article*

376

377 The structure of this article is as follows: Section 2 describes PPFM models for probabilistic
378 price forecasts and the methodology, mainly in terms of the NW-KDE approach. Section 3 contains a
379 description of the time framework and data for the PPFM models in the real-life case study. The
380 application of such PPFM models and the corresponding results are presented in Section 4. After the
381 results, Section 5 proceeds to discuss them and depicts comparisons of performances of PPFM models
382 from the point of view of MAE values and Reliability Indicator values. Finally, the conclusions of this
383 article are presented in Section 6.

384

385 **2. Probabilistic price forecasting models (PPFM models)**

386

387 The probabilistic forecasting models (PPFM models) presented in this article are based on the
388 Nadaraya–Watson Kernel Density Estimator (NW-KDE), the fundamentals of which were proposed
389 by Nadaraya and Watson [57, 58]. A KDE approach is a non-parametric approach to estimate the PDF
390 of a random variable. KDE methods have been applied satisfactorily to obtain wind and solar power
391 probabilistic forecasts [59-61].

392

393 The NW-KDE mathematical method used in our work is more complex than other KDE
394 approaches, with the main difference being that it allows the parameter values of the PDF of a Beta
395 distribution for the output variable (hourly price variable) to be obtained directly from the expected
396 and variance values, calculated basically by the applying the NW-KDE approach to the historic data
397 of explanatory price variables and the historic data of hourly prices. In this way, such PDF functions
398 allow useful probabilistic quantitative information of the price variable behavior for each hour of the
399 forecasts to be determined.

400

401 The NW-KDE method was implemented in a novel NW-KDE probabilistic forecasting tool
402 developed specifically for this research work, which also considered diverse advanced features.
403 However, only essential aspects of the NW-KDE method used in the PPFM models are presented in
404 this article due to reasons of simplicity.

405

406 In this Section 2, a mathematical description of PPFM models is presented; later the kernel
407 density estimation function utilized in these models is explained; and, lastly, parameters related to
408 probabilistic price forecasting models are described.

409

410 *2.1. Mathematical description of probabilistic price forecasting models*

411

412 Probabilistic price forecasting models consider a historical dataset composed of n cases,
413 corresponding to past instants p ($p = 1, 2, \dots, n$), of m price explanatory variables, x , and the
414 corresponding dependent variable (hourly electricity price variable, y). This set of n historical cases,

415 composed by hourly time series of the mentioned variables, constitutes the knowledge base dataset
 416 (matrix of knowledge) represented in (1).

417

$$418 \quad \left\{ \begin{array}{cccc} x_{1,1} & \dots & x_{v,1} & \dots & x_{m,1} & y_1 \\ \vdots & & \ddots & & \vdots & \vdots \\ x_{1,p} & & x_{v,p} & & x_{m,p} & y_p \\ \vdots & & & & \vdots & \vdots \\ x_{1,n} & \dots & x_{v,n} & \dots & x_{m,n} & y_n \end{array} \right\} \quad (1)$$

419
 420 The PPFM models assume that the neighborhood of a future generic case $\{x_{1,new}, \dots, x_{v,new}, \dots,$
 421 $x_{m,new}\}$ for a future hour (*new*) can be assessed for each explanatory variable (dimension) v , by a
 422 kernel density estimation function $K_v(x_{v,p}; x_{v,new}, h_v)$, where $x_{v,new}$ plays the role of the parameter of the
 423 center of the kernel function and h_v corresponds to its bandwidth, that is, the width of activation of the
 424 kernel function in the neighborhood of the *new* case for the variable v . The kernel function $K_v(x_{v,p};$
 425 $x_{v,new}, h_v)$ is a grade function, used to “select” mainly historical cases with values $x_{v,p}$ relatively “close”
 426 to each specified value of the variable $x_{v,new}$, by “activation values” given by such kernel function. The
 427 “join activation” for all dimensions, that is, for all explanatory variables, corresponds to the product
 428 of the kernel functions in all dimensions v , computed by the expression $\prod_{v=1}^m K_v(x_{v,p}; x_{v,new}, h_v)$, that is, a
 429 product kernel [62, 63].

430 In order to gain a better understanding of the mathematical description of the PPFM models,
 431 an illustrative example is included in Fig. 1. Let us consider, for simplicity, that there is only one price
 432 explanatory variable ($v=1$), the power demand variable. In Fig. 1 the price explanatory variable has a
 433 value of 40.5 GWh for a future case (value x_{new}). A suitable kernel density estimation function (for
 434 example, the one shown in the figure) will be used to assess the neighborhood of x_{new} considering the
 435 historic dataset. As shown in Fig. 1, for such value of x_{new} , a limit value $x_{new,max}$ of 42.5 GWh and a
 436 limit value $x_{new,min}$ of 38 GWh can be adequately determined (by using an appropriate basic level of
 437 activation of the kernel density estimation function), for purposes of practical computations to be
 438 carried out later. These limits of the explanatory variable values lead to determine limits of the price
 439 values between $y_{new,max}$ (32.2 €/MWh) and $y_{new,min}$ (16.0 €/MWh).

440
 441 Coming back to the PPFM models, for the general situation of m explanatory variables and a
 442 *new* generic case $\{x_{1,new}, \dots, x_{v,new}, \dots, x_{m,new}\}$ for a future instant, let us consider that the element $[Y_{new}]$
 443 , associated to the variable y_{new} (hourly price variable) in the interval $[y_{new,min}; y_{new,max}]$, is converted
 444 to the element $[Y'_{new}]$ referred to a variable y'_{new} between 0 and 1 by a regular min-max standardization.

445
 446 The expected value of $[Y'_{new}]$, for a *new* (future) instant, can be estimated by the weighted
 447 average of all values y'_p between 0 and 1 (corresponding to historical values y_p belonging to the
 448 interval $[y_{new,min}; y_{new,max}]$), where the weights are the kernel activation values (“join activation”
 449 values).

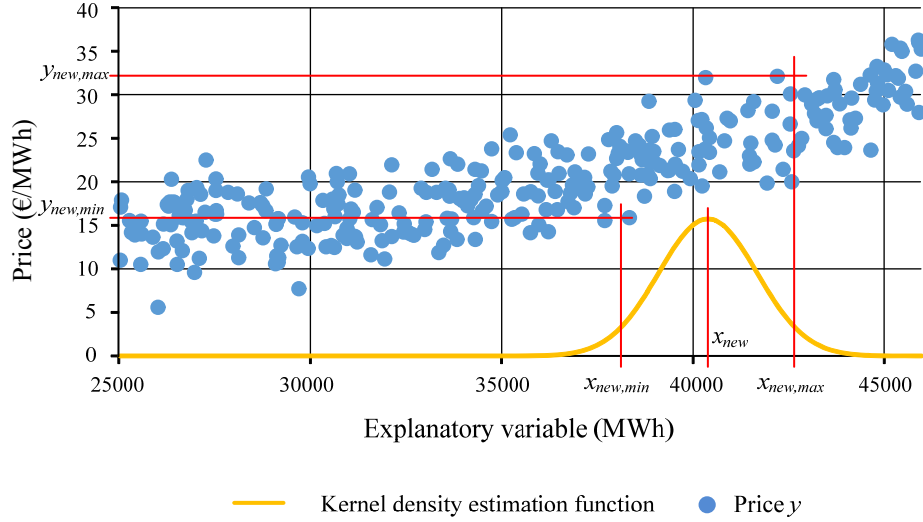


Fig. 1. Illustrative example.

Let us consider that the element $[X_{new}]$ is associated to v price explanatory variables $x_{v,new}$. The expected value of $[Y'_{new}]$ is the conditional expected value $E[Y'_{new}|X_{new}]$ that can be estimated by (2), [63],

$$E[Y'_{new}|X_{new}] = \frac{\sum_{p=n-new,min}^{n-new,max} \left(y'_p \cdot \prod_{v=1}^m K_v(x_{v,p}; x_{v,new}, h_v) \right)}{\sum_{p=n-new,min}^{n-new,max} \left(\prod_{v=1}^m K_v(x_{v,p}; x_{v,new}, h_v) \right)} \quad (2)$$

where the number $n-new,min$ is related to $y_{new,min}$ and the number $n-new,max$ is related to $y_{new,max}$.

The approach used to represent $[Y'_{new}]$, standardized in the interval $[0,1]$, allows us to obtain estimation values of the parameters α_{new} and β_{new} of the corresponding probability density function of a Beta distribution, as explained later, by using the value of $E[Y'_{new}|X_{new}]$ according to (2), and the variance $V[Y'_{new}|X_{new}]$ according to (3), [64].

$$V[Y'_{new}|X_{new}] = E[(Y'_{new})^2|X_{new}] - (E[Y'_{new}|X_{new}])^2 \quad (3)$$

Thus, the application of the NW-KDE method to the expected value of the square of the dependent variable $E[(Y'_{new})^2|X_{new}]$ and to the square of the expected value $(E[Y'_{new}|X_{new}])^2$, leads to obtain the variance $V[Y'_{new}|X_{new}]$ that can be estimated by (4).

$$V[Y'_{new}|X_{new}] = \frac{\sum_{p=n-new,min}^{n-new,max} \left((y'_p)^2 \cdot \prod_{v=1}^m K_v(x_{v,p}; x_{v,new}, h_v) \right)}{\sum_{p=n-new,min}^{n-new,max} \left(\prod_{v=1}^m K_v(x_{v,p}; x_{v,new}, h_v) \right)} - \left(\frac{\sum_{p=n-new,min}^{n-new,max} \left(y'_p \cdot \prod_{v=1}^m K_v(x_{v,p}; x_{v,new}, h_v) \right)}{\sum_{p=n-new,min}^{n-new,max} \left(\prod_{v=1}^m K_v(x_{v,p}; x_{v,new}, h_v) \right)} \right)^2 \quad (4)$$

473
 474 The probability density function $f(y'_{new}; \alpha_{new}, \beta_{new})$ of a Beta distribution supported in the
 475 interval $[0,1]$, for y'_{new} in the interval $[0,1]$, is given by (5), [65, 66],

$$476 \quad f(y'_{new}; \alpha_{new}, \beta_{new}) = \frac{1}{B(\alpha_{new}, \beta_{new})} y'^{\alpha_{new}-1} \cdot (1-y')^{\beta_{new}-1} \quad (5)$$

478
 479 where $B(\alpha_{new}, \beta_{new})$ is a known normalization “constant” (if fixed values of $\alpha_{new}, \beta_{new}$) [65], and the
 480 estimated values of the parameters α_{new} and β_{new} , corresponding to the *new* instant, are obtained from
 481 (6) and (7) using the method of moments [65].

$$482 \quad \alpha_{new} = \frac{(1-E[Y'_{new}|X_{new}]) \cdot (E[Y'_{new}|X_{new}])^2}{V[Y'_{new}|X_{new}]} - E[Y'_{new}|X_{new}] \quad (6)$$

$$483 \quad \beta_{new} = \alpha_{new} \cdot \frac{(1-E[Y'_{new}|X_{new}])}{E[Y'_{new}|X_{new}]} \quad (7)$$

486
 487 The expected value of the hourly price, i.e., the point forecast of hourly price value, with prices
 488 values expressed in €/MWh in the interval $[y_{new,min}; y_{new,max}]$, can be obtained by using a probability
 489 density function $f_{new}(y_{new}; \alpha_{new}, \beta_{new}, y_{new,min}; y_{new,max})$ of a Beta distribution, supported in such interval
 490 $[y_{new,min}; y_{new,max}]$, where y_{new} represents the variable associated to the hourly price. Thus the expected
 491 value of the hourly price is given by (8), [65, 66].

$$492 \quad y_{new,min} + (y_{new,max} - y_{new,min}) \frac{\alpha_{new}}{\alpha_{new} + \beta_{new}} \quad (8)$$

494
 495 Lastly, a variety of useful quantitative probabilistic information can be also obtained from the
 496 mentioned probability density function for the price forecast, as presented in Section 4.2.

497 498 2.2. Kernel density estimation function

499
 500 Different kinds of kernel functions can be used. The Gaussian function is the most common
 501 and practical function to be applied to each dimension (each explanatory variable) v by (9).

502

503
$$K_v(x_{v,p}; x_{v,new}, h_v) = \frac{1}{h_v \sqrt{2\pi}} e^{-\frac{(x_{v,p} - x_{v,new})^2}{2h_v^2}} \quad (9)$$

504

505 Notice that $x_{v,p}$ plays the role of the independent variable in the kernel Gaussian function K_v
 506 $(x_{v,p}; x_{v,new}, h_v)$ and $x_{v,new}$ and h_v acts as parameters. There is one kernel function for each variable v ,
 507 and it is applied to each value $x_{v,p}$ of the historical cases.

508

509 Observe that $x_{v,new}$ is set as the center of the Gaussian function that is used to assess the
 510 neighborhood of $x_{v,new}$ (i.e., mainly historical cases p with values $x_{v,p}$ relatively “close” to $x_{v,new}$).
 511 Furthermore h_v is the Gaussian RMS width, or the Gaussian standard deviation parameter, and it
 512 represents the bandwidth of the kernel.

513

514 *2.3. Parameters related to probabilistic price forecasting models*

515

516 As mentioned at the beginning of this Section 2, the NW-KDE method was implemented in a
 517 novel NW-KDE probabilistic forecasting tool, which contains diverse parameters. Some of these
 518 parameters have to be calibrated in order to achieve an adequate performance of the PPFM models.

519

520 First, descriptions of parameters are provided (Section 2.3.1); and afterwards, a summary of a
 521 complex procedure of bandwidths calibration is briefly outlined to obtain satisfactory values of
 522 bandwidths (Section 2.3.2).

523

524 *2.3.1. Descriptions of parameters*

525

526 When working with a kernel estimator it is necessary to select the kernel function K_v and the
 527 smooth parameter or bandwidth h_v , for each explanatory variable (dimension v). The selection of K_v is
 528 a relatively less important problem, since different kernel functions that produce good results, can be
 529 utilized. In this article, the Gaussian kernel density function is applied as previously indicated in
 530 Section 2.2. An inconvenience of dealing with the Gaussian kernel density function is that if it is not
 531 limited, then it requires intensive computation for the historical dataset of cases shown in (1). In order
 532 to accelerate the forecasting computation, a parameter called standardized basic level of activation is
 533 introduced (in the probabilistic price forecasting models), bla_{std} , for a standardized function, $K_{v,std}$,
 534 which corresponds to the function K_v multiplied by $h_v \sqrt{2\pi}$. Thus, the basic level of activation, bla ,
 535 which corresponds to bla_{std} divided by $h_v \sqrt{2\pi}$, defines the minimum level of activation in the Gaussian
 536 kernel function K_v . Theoretically the parameter bla_{std} could be a value between 0 and 1, with a wide
 537 knowledge base activation for low values of bla_{std} and straiten knowledge base activation for values
 538 close to 1. The value of bla_{std} , or the corresponding bla , defines the values of x_{v,new_min} and x_{v,new_max}
 539 by using the inverse of the cumulative distribution function CK_v , of the Gaussian kernel function K_v ,
 540 through (10) and (11).

541

542
$$x_{v,new_min} = CK_v^{-1}(bl_a; x_{v,new}, h_v) \quad (10)$$

543
$$x_{v,new_max} = CK_v^{-1}((1-bl_a); x_{v,new}, h_v) \quad (11)$$

544

545

546

547

548

549

550

551

552

553

554

555

In comparison with the selection of the type of kernel function, the choice of the bandwidths, h_v (for each explanatory variable v), is more important because if the bandwidth values are relatively small, then we will obtain an underestimation of the dispersion of the estimated uncertainty of probabilistic price forecasts, with a risk of over-fitting the expected value of the hourly price (i.e., the point forecast of hourly price value) obtained from the probabilistic forecast. On other hand, if the bandwidth values are relatively large, then the dispersion of the estimated uncertainty will be excessively wide, with poor accuracy for the uncertainty of probabilistic forecasts and also for the expected value of the hourly price. The optimal bandwidth for each explanatory variable would be the one that would optimize a suitable indicator of uncertainty of probabilistic price forecasts. We select the *RI* (Reliability Indicator), presented later in Section 4.3.

556

557

558

559

560

561

562

The NW-KDE probabilistic forecasting tool can be applied with a dynamic iterative process to seek a value of the bandwidth h_v , for each explanatory variable v , which achieves a good value (near the optimal value) of the indicator of uncertainty of probabilistic forecast in the neighborhood of a new case $\{x_{1,new}, \dots, x_{v,new} \dots, x_{m,new}\}$. This dynamic iterative calibration process starts from relatively large bandwidth values, and if the indicator value improves during such a process, then all bandwidths are decreased, as described in Section 2.3.2, by using a factor F_{chg} , belonging to the interval $[0,1]$.

563

564

565

566

567

568

569

570

571

572

An inconvenience of this dynamic iterative process would be that in some situations, the decrease of bandwidths could be excessive when activating only a very small or null number of points (cases), which would create a mathematical problem of statistical representativeness with poor representation of the probabilistic forecasting output. This inconvenience would be particularly important if the historical dataset of cases is small or if the number of explanatory variables is very large. In order to avoid this inconvenience, the NW-KDE probabilistic forecasting tool sets a parameter called “number of points”, N_p , which corresponds to the minimum number of activated points from the historical dataset of cases shown in (1), tolerable to be statistically representative for probabilistic forecasts.

573

574

2.3.2. Calibration of bandwidths

575

576

577

578

The calibration (optimization) of bandwidths h_v is carried out for each new case, basically by adjusting bandwidths for a region in the neighborhood of such a case $\{x_{1,new}, \dots, x_{v,new} \dots, x_{m,new}\}$, by following the stages:

579

580

581

582

Stage 1.- The iterative process starts by using a relatively large bandwidth defined for each dimension (explanatory variable v), that is 10% of $(x_{v,max} - x_{v,min})$, where $x_{v,max}$ represents the maximum value of x_v of the historical dataset of cases shown in (1) and $x_{v,min}$ represents the minimum value of such x_v .

583

584 Stage 2.- With the already defined parameters and the current values of the smoothing parameters
585 (bandwidths), the NW-KDE probabilistic forecasting tool is applied to the historical dataset of
586 cases (the historical dataset was indicated in (1)), which determines a set of activated points,
587 named the “forecast set”.

588

589 Stage 3.- There is a verification of the number of activated points, in accordance with the
590 following conditions:

591

592 3.1.- If it is lower than N_p , then all the values of h_v are enlarged by the factor F_{chg} , that is, the
593 resulting enlarged values are $h_v \cdot (1 + F_{chg})$. Afterwards, return to Stage 2.

594

595

3.2.- If it is not lower than N_p , then continue to Stage 4.

596 Stage 4.- In the “forecast set”, select the N_p points that are the “closest ones” to the new case, that
597 is, the N_p points with the highest value of the “joint activation” computed by the expression

598 $\prod_{v=1}^m K_v(x_{v,p}; x_{v,new}, h_v)$. This set of N_p points is named the “validation set” and obviously it is a subset

599

of the “forecast set”.

600

601 Stage 5.- By applying equations (6) and (7) to the “forecast set”, compute the parameters α and
602 β of the “output forecast” for the new case. From this stage, the “output parameters” (α_{new} , β_{new} ,
603 $y_{new,min}$, $y_{new,max}$) are obtained.

604

605 Stage 6.- For each case k of the “validation set”, obtained in Stage 4, calculate the fitness of the
606 historical value (y_k) in the “output forecast” which is represented by the parameters (α_{new} , β_{new} ,
607 $y_{new,min}$, $y_{new,max}$). The fitness value is computed by using the Beta cumulative distribution function
608 $F_{new}(\alpha_{new}, \beta_{new}, y_{new,min}, y_{new,max})$, which obtains a value in the interval $[0,1]$. Afterwards, the
609 fitness values of the N_p cases in the “validation set” are used to determine the value of the RI
610 (Reliability Indicator), via the process presented in Section 4.3.

611

612 6.1.- If it is the first iteration or if the value of the RI , for the “validation set”, is better than the
613 one obtained in the previous iteration, then all the values of h_v are reduced by the factor F_{chg} ,
614 that is, the resulting reduced values are $h_v \cdot (1 - F_{chg})$. Afterwards, return to Stage 2.

615

616 6.2.- If it is not the first iteration and if the value of the RI , for the “validation set”, does not
617 improve with regards to the one of the previous iteration, then the process of calibration
618 finishes.

618

619 A simplified flow chart of the proposed methodology associated to the development of the
620 PPFM models is shown in Fig. 2.

621

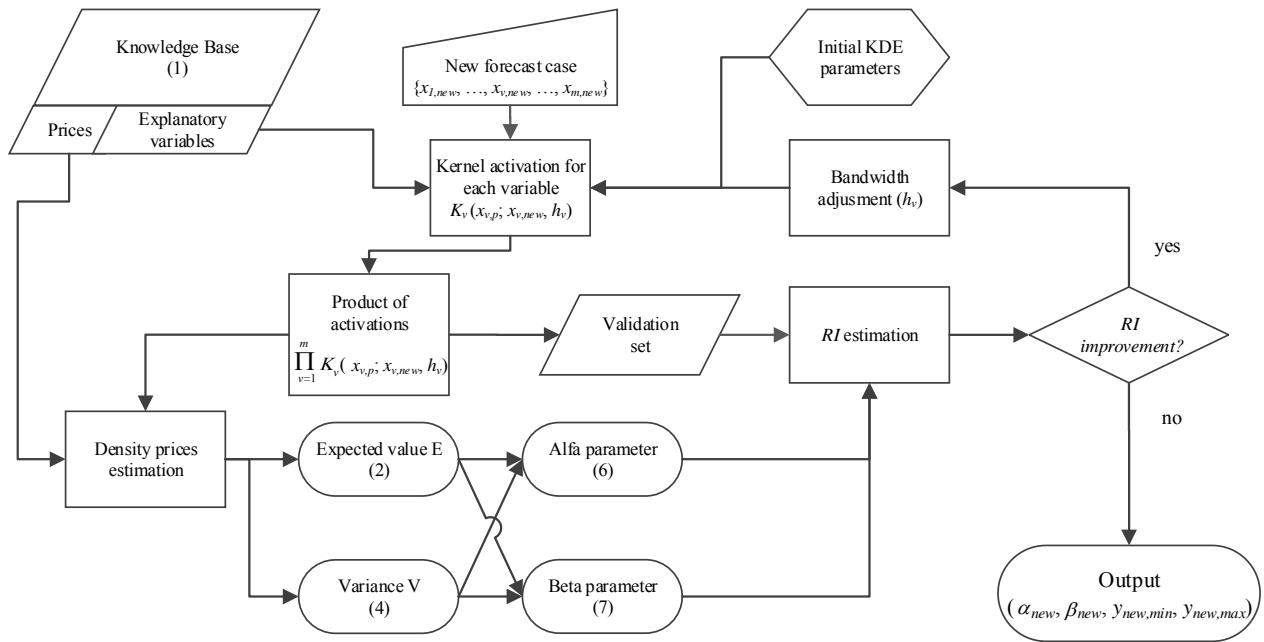


Fig. 2. Simplified flow chart of the proposed methodology associated to the development of the PPFM models.

622

623 3. Time framework and data for probabilistic price forecasting models

624 As abovementioned in Section 1, the real-life case study of the Iberian Electricity Market
 625 (MIBEL) was used to satisfactorily test the PPFM models, although these models can be applied to
 626 any other day-ahead electricity market. The MIBEL comprises different markets: the derivatives
 627 exchange market, managed by the company OMIP [67], and the daily and intraday markets, both
 628 managed by the company OMIE [68]. The daily market is a marginal auction market structured in a
 629 daily session, where next-day hourly sale and electricity purchase transactions are carried out.

630

631 Section 3.1 describes the time framework for the PPFM models. And afterwards, data
 632 corresponding to the real-life case study for PPFM models is shown in Section 3.2.

633 3.1. Time framework for probabilistic price forecasting models

634 PPFM models use input (price explanatory) variables that correspond to recorded hourly time
 635 series. Fig. 3 shows the time framework used for PPFM models. The day-ahead hourly price forecast
 636 $\hat{p}_{D+1,h|D,t}^d$ for each hour h of the 24 hours in day $D+1$ (output in Fig. 3) is obtained at hour t of the day
 637 D . This hour t of day D can be any moment before the closing of the daily market session and after the
 638 instant in which the variables corresponding to forecasted wind power generation and forecasted
 639 demand for the day $D+1$ are known.

640

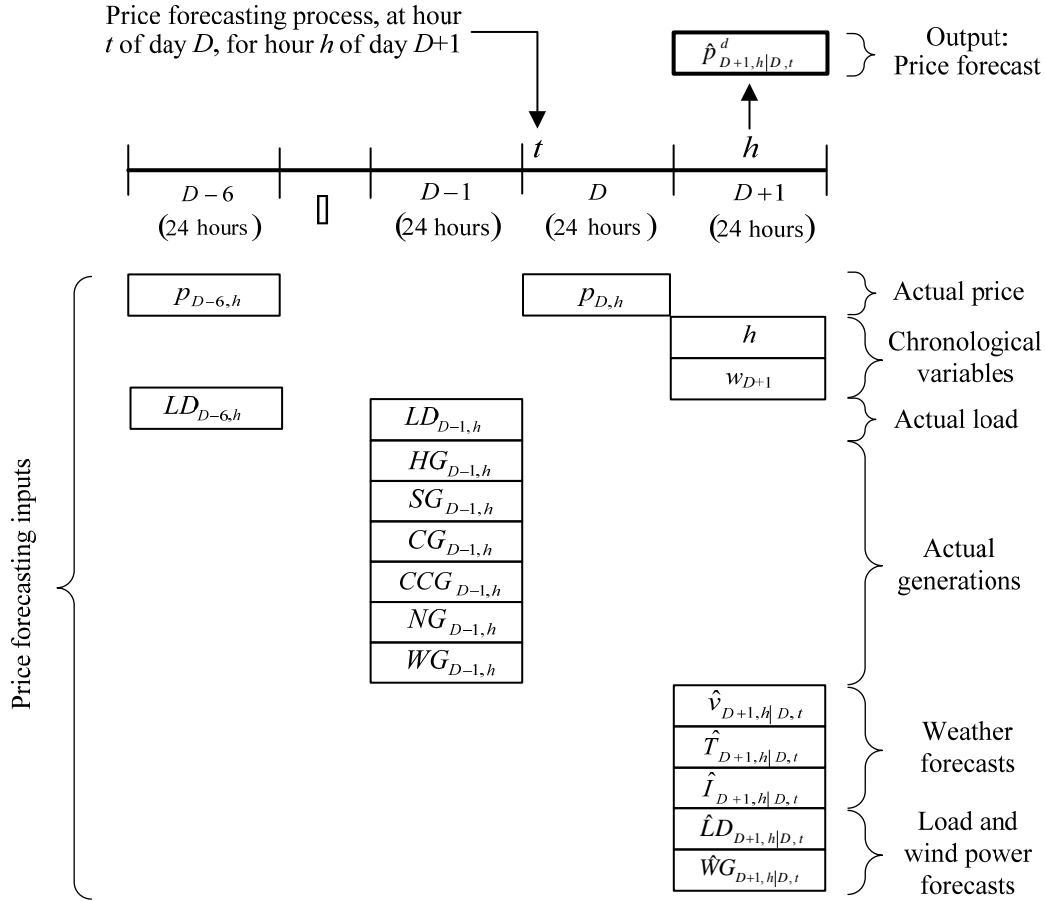


Fig. 3. Time framework of probabilistic price forecasting models.

641
642

643 The price $p_{D-6,h}$ for hour h of day $D-6$, and the price $p_{D,h}$ for hour h of the day D , are inputs to
 644 forecast the price for the hour h of day $D+1$. Inputs are also the day of the week w_{D+1} , the hour h of
 645 day $D+1$, and the weather forecasts for hour h of day $D+1$ (obtained at the first hours of day D for the
 646 geographical region corresponding to the electric power market), that is, regional weighted forecasted
 647 hourly temperatures $\hat{T}_{D+1,h|D,t}$, regional weighted forecasted hourly irradiances $\hat{I}_{D+1,h|D,t}$ and regional
 648 weighted forecasted hourly wind speeds $\hat{v}_{D+1,h|D,t}$.

649

650 Fig. 3 also includes other diverse inputs: hydropower generation $HG_{D-1,h}$, solar power
 651 generation and power cogeneration $SG_{D-1,h}$, coal power generation $CG_{D-1,h}$, combined cycle power
 652 generation $CCG_{D-1,h}$, wind power generation $WG_{D-1,h}$, nuclear power generation $NG_{D-1,h}$ and power
 653 demand $LD_{D-1,h}$ at hour h of day $D-1$; power demand $LD_{D-6,h}$ at hour h of day $D-6$; and wind power
 654 generation forecast $\hat{W}G_{D+1,h|D,t}$ and power demand forecast $\hat{L}D_{D+1,h|D,t}$ for hour h of day $D+1$.

655 3.2. Data for probabilistic price forecasting models

656 Different kinds of data have been considered for development of PPFM models. The data is as
 657 follows:

658

659 a. Chronological data (hour, day of the week).

- 660 b. Actual hourly data prices of the electricity market (MIBEL), available from the market operator
661 OMIE [68].
- 662 c. Actual hourly data of the power system: power demand, hydropower generation, wind power
663 generation, cogeneration and solar power generation, coal power generation, nuclear power
664 generation, combined cycle power generation and power exchanged with France. This data was
665 obtained by aggregating a very large amount of information from the websites of REE, the Spanish
666 Transmission System Operator (TSO) [69], and REN, the Portuguese TSO [70].
- 667 d. Data of hourly forecasts of the power system: wind power generation forecasts and power demand
668 forecasts. These forecasts were obtained by aggregating forecast information from the mentioned
669 TSOs.
- 670 e. Data of hourly weather forecasts: weighted average temperature, solar irradiance and wind speed.
671 These forecasted values were obtained with the NWP (Numerical Weather Prediction) mesoscale
672 model WRF NMM [71], initialized with the forecasts provided by the global NWP model GFS
673 [72]. The weighted average temperature was obtained as a weighted average of the temperature
674 forecast for near to 250 points covering the main demand points in all the regions of the Iberian
675 Peninsula (Spain and Portugal); the weights were proportional to the aggregated power demands
676 of each region. Similarly, the weighted average solar irradiance and wind speed were obtained as
677 the weighting average of hourly solar irradiances and wind speeds in nearly 750 points covering
678 all regions of the Iberian Peninsula; in this case the weights were proportional to the regional
679 installed capacity in solar based plants and in wind farms, respectively.

680
681 The set of price explanatory variables of the PPFM models is shown in Table 1. This set
682 includes variables of the five kinds of data described above.

683
684

Table 1. Price explanatory variables of PPFM models.

Variable	Description
V1	hour
V2	week day
V3	hourly price D
V4	hourly price $D-6$
V5	hourly power demand $D-1$
V6	hourly power demand $D-6$
V7	forecasted hourly power demand $D+1$
V8	forecasted hourly temperature $D+1$
V9	forecasted hourly wind speed $D+1$
V10	forecasted hourly irradiance $D+1$
V11	forecasted hourly wind power generation $D+1$
V12	hourly wind power generation $D-1$
V13	hourly hydropower generation $D-1$
V14	hourly cogeneration and solar power generation $D-1$
V15	hourly coal power generation $D-1$
V16	hourly nuclear power generation $D-1$
V17	hourly combined cycle power generation $D-1$

686

687

688

689

690

691

692

693

694

695

696

697

698

699

700

701

702

703

704

705

The data corresponds mainly to years 2012 and 2013. It was divided into an in-sample dataset, used to create PPFM models and an out-sample dataset used for testing them. In order to have a good representation of the different price behaviors along the year, the out-sample dataset was composed of complete weeks extracted along the two years of data. The in-sample and out-sample datasets were defined as follows:

- i. In-sample dataset: all the hours of the days in 2012 (from February 2nd) and 2013 (to December 4th), except those included in the out-sample dataset, totaling 13512 cases (hours). This in-sample dataset corresponds to the knowledge base dataset represented in (1).
- ii. Out-sample dataset: all the hours of the weeks with numbers 5, 10, 15, 20, 25, 30, 35, 40, 45, 50 in 2012, and weeks number 2, 7, 12, 17, 22, 27, 32, 37, 42, 47 in 2013; a total of 3360 cases (hours).

The in-sample and out-sample datasets were characterized by similar statistical parameters.

4. Application of probabilistic price forecasting models and results

706 Probabilistic price forecasting models (PPFM models) were applied to the abovementioned
707 real-life case study using combinations of the explanatory variables of Table 1 and the data presented
708 in Section 3.2.
709

710 In this Section 4, a summary of input variable selection studies for PPFM models are presented
711 in order to determine the best combination of input variables that leads to the best PPFM model with
712 the lowest Mean Absolute Error (MAE) value; later, detailed results of the best PPFM model for hourly
713 price forecasts are described; lastly a Reliability Indicator (*RI*) is introduced to assess the uncertainty
714 of probabilistic price forecasts: the *RI* provides a quantitative measure (between 0% and 100%) of
715 “reliability” of the forecasts provided by the PPFM models.
716

717 *4.1 Selection of input variables for probabilistic price forecasting models*

718

719 A summary of variable selection studies for PPFM models is shown in this Section,
720 corresponding to reasonable combinations of input variables (grouped by their common
721 characteristics) in order to find the best PPFM model that corresponds to the input variable
722 combination that achieves the lowest Mean Absolute Error value.
723

724 The error indicator Mean Absolute Error (MAE) was calculated, for probabilistic forecasting
725 models, according to (12),
726

$$727 \quad \text{MAE} = \frac{1}{N} \sum_{T=1}^N |P_{forecast_T} - P_{real_T}| \quad (12)$$

728

729 where N is the number of elements (or number of forecasting hours) in the out-sample dataset, P_{real_T}
730 is the real hourly price value for the hour T , and $P_{forecast_T}$ is the expected value of hourly price (point
731 forecast of hourly price) of the PPFM model for the hour T .
732

733 The MAE errors for PPFM models (PPFM1 to PPFM23), with different input variables, are
734 presented in Table 2. The values of the Reliability Indicator of Table 2 will be commented upon later.
735 The selection of variables follows an ordered analysis, such that only some PPFM models are presented
736 in the table for conclusive purposes. The construction of Table 2 corresponds to a selection process
737 with the following sequence:
738

- 739 a. Models PPFM1 to PPFM3 for chronologic variables selection;
 - 740 b. Models PPFM4 to PPFM6 for price variables selection;
 - 741 c. Models PPFM7 to PPFM10 for power demand and forecasted power demand variables
742 selection;
 - 743 d. Models PPFM11 to PPFM16 for forecasted weather and forecasted wind generation
744 variables selection; and
 - 745 e. Models PPFM17 to PPFM23 for power generation variables selection.
- 746

747 Models PPFM1 and PPFM2 are two first elemental models that lead the highest MAE errors
 748 of the studied models shown in Table 2. PPFM3 is a simple baseline model with a MAE error value
 749 of 9.01 €/MWh.
 750
 751
 752

Table 2. PPFM models and their MAE and Reliability Indicator values.

Type of variables	Model	V1	V2	V3	V4	V5	V6	V7	V8	V9	V10	V11	V12	V13	V14	V15	V16	V17	MAE (€/MWh)	Reliability indicator (%)
Chronologic	PPFM1	X																	9.78	78.51
	PPFM2		X																10.40	75.25
	PPFM3	X	X																9.01	82.51
Price	PPFM4	X	X	X															7.73	80.61
	PPFM5	X	X		X														9.09	79.33
	PPFM6	X	X	X	X														7.70	82.38
Demand	PPFM7	X	X	X	X	X													7.58	80.92
	PPFM8	X	X	X	X		X												7.60	81.86
	PPFM9	X	X	X	X			X											7.57	81.21
	PPFM10	X	X	X	X	X		X											7.48	82.98
Weather	PPFM11	X	X	X	X	X	X	X											7.48	83.61
	PPFM12	X	X	X	X	X	X		X										6.16	83.39
	PPFM13	X	X	X	X	X	X			X									7.52	83.17
	PPFM14	X	X	X	X	X	X	X	X										6.04	84.92
Power Generation	PPFM15	X	X	X	X	X	X	X	X			X							5.81	83.53
	PPFM16	X	X	X	X	X	X	X				X							5.65	85.07
	PPFM17	X	X	X	X	X	X	X				X	X						5.59	84.47
	PPFM18	X	X	X	X	X	X	X				X		X					5.58	85.25
	PPFM19	X	X	X	X	X	X	X				X			X				5.63	84.84
	PPFM20	X	X	X	X	X	X	X				X				X			5.62	85.75
	PPFM21	X	X	X	X	X	X	X				X					X		5.60	84.11
	PPFM22	X	X	X	X	X	X	X				X						X	5.62	83.65
	PPFM23	X	X	X	X	X	X	X				X	X	X	X	X			5.55	85.64

753
 754 If variable V3 (hourly price *D*) is added to those used by model PPFM3, leading to model
 755 PPFM4, then the MAE error decreases to 7.73 €/MWh; and model PPFM6 obtains an error of 7.7
 756 €/MWh when including the price *D*-6 variable (V4) in model PPFM4.
 757

758 The inclusion of variable V5 (hourly power demand *D*-1) in model PPFM6 slightly reduces the
 759 MAE error to 7.58 €/MWh (model PPFM7). Additionally, if variable V7 (hourly forecasted power

760 demand $D+1$) is included in model PPFM7, the MAE error is reduced to 7.48 €/MWh (model
761 PPFM10).

762

763 From the point of view of the set of models PPFM11 to PPFM14, compared to model PPFM10,
764 the forecast wind speed variable (V9) in model PPFM12 obtains a MAE error of 6.16 €/MWh.
765 Furthermore adding the forecasted temperature variable (V8) in model PPFM14 leads to a slightly
766 better error of 6.04 €/MWh.

767

768 The forecasted wind power variable (V11) added to model PPFM14 achieves an error of 5.81
769 €/MWh (model PPFM15). Since variables V9 and V11 have collinear information, the exclusion of
770 variable V9 in model PPFM15 leads to a slightly better error of 5.65 €/MWh (model PPFM16).

771

772 Models PPFM17 to PPFM22 allow the evaluation of the improvement in the MAE error by
773 adding variables V12 to V17 (power generation variables $D-1$). Variable V13 (hydropower generation
774 $D-1$) is the one that achieves a lower error, 5.58 €/MWh in model PPFM18. The inclusion of variables
775 V15 to V17 (thermal power generation $D-1$) in the previous model PPFM18 results in the best
776 performance of PPFM models (model PPFM23), reaching a MAE error value of 5.55 €/MWh.
777 Therefore, among models PPFM1 to PPFM23, the best PPFM model is PPFM23.

778

779 Notice that there are five families of PPFM models (which correspond to the five families of
780 types of price explanatory variables): i) models PPFM1, PPFM2 and PPFM3, containing chronological
781 variables; ii) models PPFM4, PPFM5 and PPFM6, which include price variables (and chronological
782 ones); iii) models PPFM7 to PPFM10, which contain demand variables (and price and chronological
783 ones); iv) models PPFM11 to PPFM14, which take into account weather forecasting variables (and
784 demand, price and chronological variables); and v) PPFM15 to PPFM23, which include generation
785 variables (and weather forecasting, demand, price and chronological variables).

786

787 Lastly, observe that, from the point of view of the MAE error values in Table 2, the best model
788 among models PPFM1, PPFM2 and PPFM3 is model PPFM3. MAE errors of models PPFM4, PPFM5
789 and PPFM6 in Table 2, determine that the best model is PPFM6. The best model, upon analyzing MAE
790 errors of models PPFM7 to PPFM10, is model PPFM10. Among the models PPFM11 to PPFM14, the
791 best model is PPFM14. Lastly the best model upon studying MAE errors of models PPFM15 to
792 PPFM23, is model PPFM23. Thus, the best models of each of the five families of probabilistic price
793 forecasting models are models PPFM3, PPFM6, PPFM10, PPFM14 and PPFM23.

794

795 *4.2 Results of the best probabilistic price forecasting model PPFM23*

796

797 Values of the input variables used in model PPFM23 (the best probabilistic price forecasting
798 model among models PPFM1 to PPFM23) for three forecasts of hourly price are shown in Table 3, as
799 well as output (results) values, quantiles and the real price values. First forecast (Forc1) corresponds
800 to the nineteenth hour on a Sunday (18:00 to 18:59 on May 26th, 2013), on a day without significant
801 renewable generation but with relatively low prices on the previous day, resulting in a normal price at

802 a time like this on a Sunday. Second forecast (Forc2) refers to the twenty-third hour on a Thursday
 803 (22:00 to 22:59 on May 30th, 2013), on a working day but with significant wind and hydro generation,
 804 resulting in a relatively low price at a time like this on a Thursday. Third forecast (Forc3) was obtained
 805 for the eleventh hour on a Monday (10:00 to 10:59 on October 14th, 2013), on a working day with low
 806 wind and hydro generation and with relatively high prices on previous days, resulting in a high price
 807 at a time like this on a Monday.
 808

809 Thus, the expected values of hourly price (i.e. point forecasts of price) obtained from the model
 810 PPFM23 correspond to price values that are relatively close to real prices values, since the percentages
 811 of error were 1.6%, -6.6% and -0.7% for the forecasts Forc1, Forc2 and Forc3, respectively (Table 3),
 812 in which such error percentages were calculated using the difference between expected and real price
 813 values with respect to the real ones.
 814

815 In Table 3, the variance values correspond to a comparatively higher dispersion of the
 816 probability density functions of forecasts Forc1 and Forc2, and to a relatively svelter probability
 817 density function of the forecast Forc3.
 818
 819

Table 3. Forecasts from the probabilistic price forecasting model PPFM23

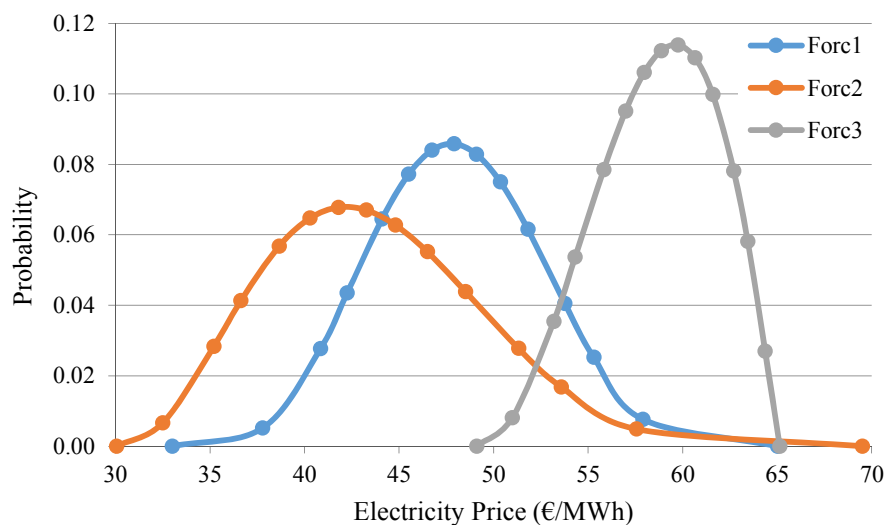
		Forc1	Forc2	Forc3
Input variables	V1 hour (0-23h)	18	22	10
	V2 week day (1-7)	1	5	2
	V3 price D (€/MWh)	30.86	46.20	74.20
	V4 price $D-6$ (€/MWh)	52.76	51.10	68.96
	V5 power demand $D-1$ (MWh)	29457	36760	26392
	V7 forecasted power demand $D+1$ (MWh)	35055	34732	36963
	V8 forecasted temperature $D+1$ (°C)	16.3	18.1	15.4
	V11 forecasted wind power $D+1$ (MWh)	7433	11979	8467
	V13 hydropower generation $D-1$ (MWh)	2093	8081	1200
	V15 coal power generation $D-1$ (MWh)	4277	4755	8017
	V16 nuclear power generation $D-1$ (MWh)	4691	4077	5994
	V17 combined cycle power $D-1$ (MWh)	1768	2029	2612
Real value	Real price (€/MWh)	47.23	46.75	59.05
Outputs	Expected value of price (€/MWh)	47.97	43.68	58.66
	Variance (€/MWh) ²	19.22	31.33	9.81
	Parameter α	5.739	3.532	3.165
	Parameter β	6.534	6.694	2.139
	Minimum price (€/MWh)	33.00	30.06	49.10
	Maximum price (€/MWh)	65.01	69.50	65.13
	Percentage error (%)	1.6	-6.6	-0.7
Quantiles	Quantile Q10 (€/MWh)	42.25	36.64	54.31
	Quantile Q25 (€/MWh)	44.83	39.50	56.42
	Quantile Q50 (€/MWh)	47.91	43.27	58.87
	Quantile Q75 (€/MWh)	51.05	47.45	61.10
	Quantile Q90 (€/MWh)	53.77	51.31	62.70

820
 821 In Table 3, values of results (parameters α and β , and maximum and minimum price) determine
 822 probability density functions (corresponding to Beta distributions), which allow a variety of useful
 823 information to be obtained, such as quantile representations and probability calculations. For instance,
 824 we can directly answer the question: “What are the probabilities that electricity prices will be higher

825 than 52 €/MWh?"; they are 19%, 8% and 98% for the forecasts Forc1, Forc2 and Forc3, respectively.
 826 These probability density functions can also be used to obtain quantiles. As such, Table 3 displays
 827 quantiles Q10, Q25, Q50, Q75 and Q90 for the three forecasts of hourly price. Observe that quantile
 828 Q50 is relatively close to the expected hourly price value. Furthermore, such quantiles are also going
 829 to be shown later, in time series representations of the forecast uncertainty, throughout two weeks (Fig.
 830 4 and Fig. 5).

831

832 Fig. 4 shows the representation of the probability density functions for the three probabilistic
 833 price forecasts Forc1, Forc2 and Forc3. The probability density function (PDF) for forecast Forc1
 834 is more symmetrical (the value of the parameter β is relatively close to that of the parameter α). On one
 835 hand, the PDF function for forecast Forc2 is slightly right tailed because of the higher value of the
 836 parameter β with respect to that of the parameter α . On other hand, the PDF function for forecast Forc3
 837 is slightly left tailed because of the higher value of parameter α in comparison with that of the
 838 parameter β . It is also possible to verify that the real values of the price are "inside" the probability
 839 density functions for these forecasts: more specifically, the real price values are situated within the
 840 percentiles 44%, 71% and 52% for forecasts Forc1, Forc2 and Forc3, respectively.
 841



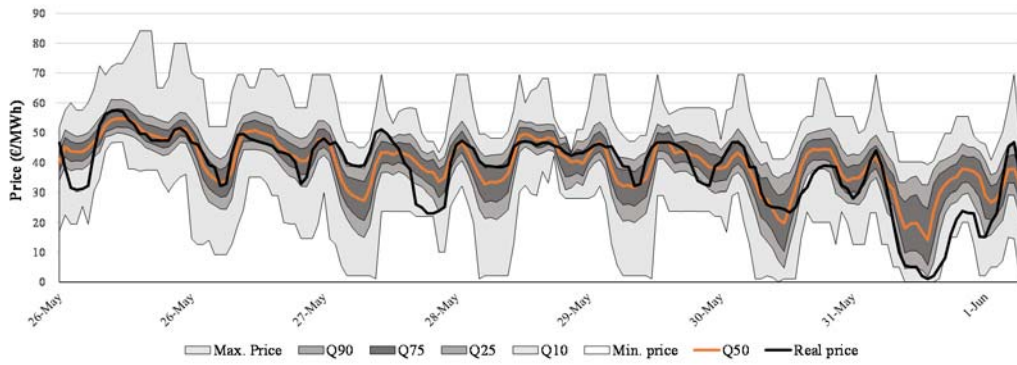
842

843

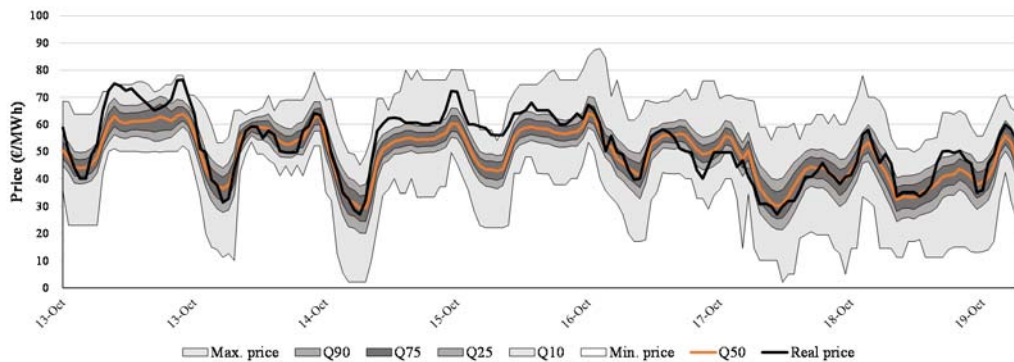
844

Fig. 4. Probability density functions for forecasts of hourly price.

845 Lastly, Fig. 5 and Fig. 6 give results (time series representations of the forecast uncertainty)
 846 from the probabilistic price forecasting model PPFM23 for week number 22 in May 2013, and for
 847 week number 42 in October 2013, showing quantiles and also real prices.
 848



849
850
851
852
Fig. 5. Probabilistic price forecasts for week number 22 in May 2013



853
854
855
856
Fig. 6. Probabilistic price forecasts for week number 42 in October 2013

857
858
4.3 Indicator of probabilistic price forecast uncertainty of PPFM models

859 The accuracy of explainable information of the forecasts of the PPFM models can be evaluated
860 based on deviations of the real price values with respect to the expected values of the hourly price
861 (point forecast of hourly price) from such models, by using appropriate performance error indicators
862 as the indicator MAE above mentioned.
863

864 Indicators of uncertainty appropriate for probabilistic price forecasts have to be able to evaluate
865 the accuracy of the forecasts of probabilistic forecasting models from the point of view of the forecast
866 uncertainty. In this aspect, a suitable reliability diagram can be used to analyze the “reliability”
867 associated to forecasts of PPFM models.
868

869 Fig. 7 shows a reliability diagram associated to an example of forecasts of the probabilistic
870 model PPFM23. In the vertical axis of the figure, the diagram gives the frequency of the events
871 (forecasted price occurrences) for the cases of the out-sample dataset, in each partition of the
872 “normalized” scale (between 0 and 1) of fitness values of price, that is shown in the horizontal axis.
873 The expected value of the hourly price, for each new case q of the out-sample dataset, is obtained by
874 using the parameters $(\alpha_{new_q}, \beta_{new_q}, y_{new_q,min}, y_{new_q,max})$ of a probability density function (PDF) of a
875 Beta distribution. Afterwards, the fitness value of the corresponding historical value of the hourly price
876 (y_q) is calculated. This fitness value is computed by using the Beta cumulative distribution function

877 $F_{new_q}(y_q; \alpha_{new_q}, \beta_{new_q}, y_{new_q,min}, y_{new_q,max})$, which obtains a value in interval $[0,1]$, to be situated in
878 the horizontal axis of Fig. 7. These fitness values are classified in the twenty partitions, with intervals
879 of 0.05. The twenty partitions presented in intervals of 0.05, on the horizontal axis of the figure, have
880 an ideal frequency (“target frequency”) of 5%. Since these partitions correspond to a bounded interval
881 $[0, 1]$, the target frequency for the two additional partitions outside such interval must be 0%. Fig. 7
882 shows that there is about 2% of price occurrences (events) in the partition corresponding to indication
883 “< MIN”, i.e. below the interval $[0, 1]$, and there is about 3% of price occurrences in the partition
884 corresponding to indication “> MAX”, i.e. above such interval. Most of the partitions between 0.05
885 and 0.35 on the horizontal axis correspond to frequencies of price occurrences that are clearly below
886 the target frequency. In the partition 0.95-1.00, obviously the frequency of price occurrences is above
887 the target frequency.

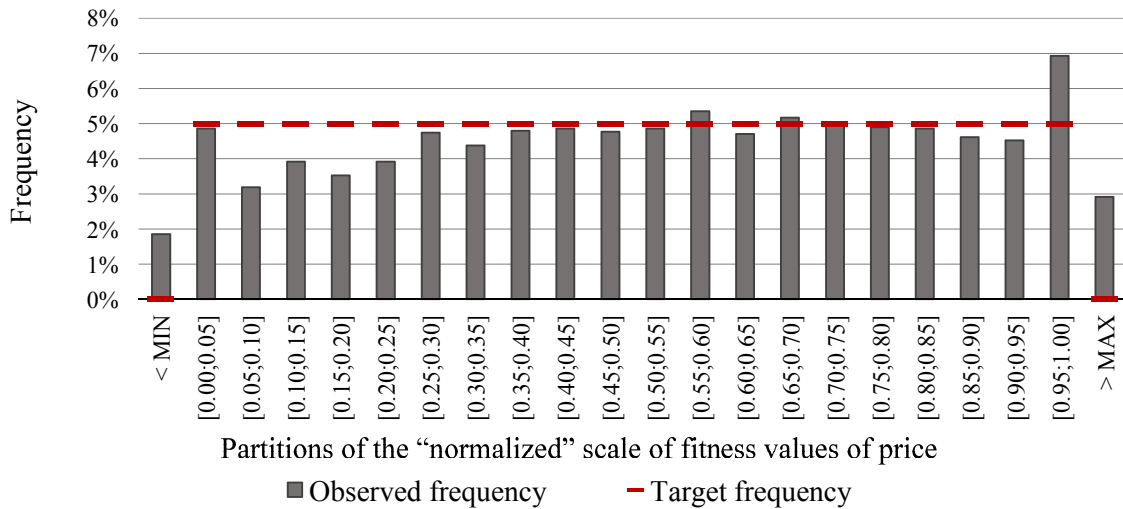
888

889 A suitable indicator to evaluate the “reliability” value associated to forecasts of PPFM models,
890 the so-called Reliability Indicator, RI , was introduced. It gives a measure related to the average
891 normalized difference between the observed frequencies and target frequency, according to (13),
892
893

$$894 \quad RI = \left(1 - \sum_{i=1}^{NQ} |f_{obs,i} - f_{tar,i}| \right) \cdot 100\% \quad (13)$$

895

896 where $f_{obs,i}$ and $f_{tar,i}$ are the observed frequencies (in per unit) and the target frequency (in per unit) for
897 the interval i ; and NQ is the total number of partitions (intervals).
898



899

900

901

Fig. 7. Reliability diagram example from the probabilistic price forecasting model PPFM23.

902

903

904

The reliability diagram of Fig. 7, obtained from an example of forecasts of the model PPFM23, corresponds to a value of the indicator RI of 84.2%. The values of the RI for probabilistic models PPFM1 to PPFM23, applied to price forecasts using the data of Section 3.2, are given in Table 2.

905 Observe that the best model PPFM23, which achieved the lowest MAE error, obtained one of the
906 highest *RI* values.

907

908 **5. Discussion**

909

910 As indicated in Section 4, probabilistic price forecasting models PPFM3, PPFM6, PPFM10,
911 PPFM14 and PPFM23, are the best models of each of the five families of PPFM models.

912

913 Fig. 8 shows values of two indicators (the MAE and the *RI*) for forecasts of the probabilistic
914 price forecasting models PPFM3, PPFM6, PPFM10, PPFM14 and PPFM23, using the data of Section
915 3.2. In Fig. 8, the MAE error improves (decreases) as more types of input variables (chronological
916 variables, price variables, power demand variables, forecasted weather variables, and power generation
917 variables) are included in PPFM models: the integration of price variables in model PPFM6 (variables
918 not included in model PPFM3) and the integration of meteorological variables in model PPFM14
919 (variables not included in model PPFM10) represent the information that causes a greater improvement
920 of the MAE indicator. The integration of demand variables in model PPFM10 (variables not included
921 in model PPFM6) constitutes the information that causes a comparatively lower improvement of the
922 MAE indicator.

923

924 Fig. 8 shows that the *RI* (indicator used to assess the uncertainty associated to probabilistic
925 price forecasts) improves as more types of explanatory input information (chronological information,
926 prices, power demands, forecasted weather information, and power generations) are included in PPFM
927 models, with the exception of the inclusion of price information in model PPFM6 (information not
928 included in model PPFM3), since in this case the *RI* does not increase. The most important
929 improvement in the *RI* is obtained when including the forecasted weather information in model
930 PPFM14 (information not included in model PPFM10).

931

932 Therefore, the MAE error values improved and the *RI* (“reliability”) values habitually also
933 improved as more types of input variables (chronological variables, price variables, power demand
934 variables, forecasted weather variables and power generation variables) were included in such PPFM
935 models.

936

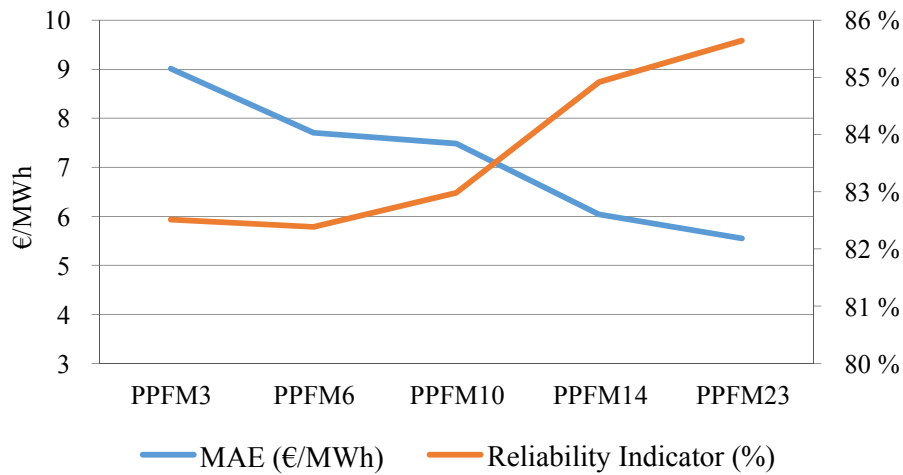


Fig. 8. Comparison of performances of probabilistic price forecasting models.

937
938
939
940

6. Conclusions

941
942
943
944
945
946

Hourly price forecasts for electric energy, in an electricity market, constitutes very useful information if known in advance, because any agent involved in such market can use such information to made strategic bids in order to maximize the associated economic profit. Furthermore, obtaining accurate price forecasts has direct impact on the producers' electric energy management. This is why electricity price forecasting has been a very active research field in the last 15 years.

947
948
949
950
951
952
953
954

Day-Ahead Electricity Price Forecasting models have been presented in the scientific literature in recent years, mostly centered on spot (point) forecasts of hourly prices, but unfortunately they can be inadequate for trading purposes because they do not show the uncertainty associated with predicted price values, that is, spot forecasts do not provide any fundamental information for risk-based market decisions. Therefore, from this point of view, probabilistic models for price forecasting overcome the limitations of spot forecasts. The most important probabilistic approaches are focused on probability density functions (PDFs). However, there is a scarcity of probabilistic approaches based on PDFs.

955
956
957
958
959
960
961
962
963
964
965
966

This article presents original Probabilistic Price Forecasting Models (PPFM models) for the day-ahead hourly probabilistic price forecasting using probability density functions of Beta distributions. The PPFM models are based on the Nadaraya–Watson Kernel Density Estimator (NW-KDE) using a suitable Gaussian KDE function for each one of its input variables, i.e., for each one of the explanatory variables of the electricity price. The new PPFM models use a very extensive set of input variables, consisting of large time series of hourly prices in previous days, regional-aggregated hourly power generations in the previous day (hydropower generation, wind power generation, solar power generation and power cogeneration, nuclear power generation, combined cycle power generation, and coal power generation), hourly power demand in the previous day, and in the previous week. Furthermore, input variables include forecasts of regional-aggregated hourly power demands, forecasts of wind power generation and weather forecasts (hourly wind speed, temperature, and irradiation) in the region for the day-ahead, as well as chronological data.

967

968 The PDF of a Beta distribution for each hour of the price variable (output variable), for each PPFM
969 model, is directly obtained from the expected and variance values associated with the NW-KDE
970 approach. Hence, the direct use of the historical input dataset (historical cases) without simplifications
971 or information losses in the knowledge base (very extensive input datasets of the PPFM models) is
972 particularly important when the purpose is to extract fundamental probabilistic information from
973 historical similar cases.

974

975 As indicated, the uncertainty representation of the output (price variable) in each forecast hour
976 of each PPFM model is given by a parametric Beta distribution defined by four parameters directly
977 obtained from the NW-KDE approach. From these Beta distribution parameters we calculate, in a
978 straightforward way, diverse types of probability values, e.g. the probabilities that electricity prices
979 will be higher or lower than a certain threshold, prediction intervals, and any kind of quantiles. The
980 aforementioned Beta PDF also provide powerful probabilistic information for risk-based decisions
981 instead of point forecasts useful only for simple decisions. In electricity market business, when the
982 market agent takes his or her decisions according to risk-based criteria, probabilistic information is
983 essential for agent decisions involving different markets or products (e.g. daily spot, intraday spot,
984 bilateral, or futures markets) with different levels of uncertainty. Parametric probabilistic price
985 forecasts, efficiently used, provide a very significant advantage for market agents implicated in risky
986 decision-making business processes, especially when high uncertainty of the prices occurs. Compared
987 to other representations of uncertainty (e.g. quantile representations), the parametric representation
988 approach used in the PPFM models of this article provides high adaptability to the risk-based analysis
989 (decision processes, based on forecasts of the PPFM models, are not conditioned by the discretization
990 of quantile representations). Furthermore, the parametric approach of Beta distributions obtained from
991 the PPFM models surpasses the simple interval representations of the uncertainty.

992

993 A new Reliability Indicator (*RI*) allows the uncertainty associated with price forecasts of each
994 PPFM model to be evaluated; i.e., the *RI* gives a quantitative measure (from 0% to 100%) of
995 “reliability” of the forecasts of each PPFM model. A suitable representation of a “reliability diagram”
996 (associated with the *RI*) is presented in this article, designed to better evaluate the performance of any
997 PDF of Beta distribution. Such suitable “reliability diagram” identifies “forecast cases” that fall outside
998 the limits of the PDF. Then, the performance of a Beta distribution can be studied directly by exploring
999 the diagram. On one hand, the *RI* provides performance comparisons of the PPFM models from the
1000 point of view of “reliability”. On the other hand, the *RI* is used in a novel procedure of bandwidths
1001 calibration, outlined below.

1002

1003 An original procedure is used to calibrate the bandwidths of the kernel Gaussian functions
1004 involved in the NW-KDE approach. The dynamic calibration process of a bandwidth is carried out by
1005 adjusting its value for each “forecast case” (“new case”), mainly based on the inputs and on the
1006 similarity of historical cases in the neighborhood of this new case to be forecast. This dynamic

1007 adjustment better (as much as possible) the bandwidths by controlling the improvement of a reliability
1008 measure given by the *RI*.

1009
1010 The new PPFM models were, for the first time, successfully applied to the real-life case of the
1011 Iberian Electricity Market (MIBEL) that covers mainland Portugal and Spain, although these PPFM
1012 models can be applied to any other day-ahead electricity market. A systematic analysis of the MAE
1013 errors of PPFM models corresponding to suitable combinations of their input variables was carried out
1014 in order to determine the best PPFM model, that is, the best combination of input variables for PPFM
1015 models that achieves the lowest MAE error value. Multiple reasonable combinations of input variables
1016 were analyzed, from simple naïve PPFM models (only with chronological input data) to much more
1017 complex PPFM models, with up to 17 input variables of data which include historical values of prices,
1018 power generations, demands, and forecasted values of demands, wind speeds, temperatures and
1019 irradiations, as well as chronological data. The best PPFM model was the model PPFM23 which
1020 included 12 of these input variables and achieved a MAE of 5.55 €/MWh.

1021
1022 The accuracy of explainable information of the forecasts of the PPFM models was evaluated
1023 by the indicator MAE; and the uncertainty of the price forecasts obtained by PPFM models was
1024 evaluated by the *RI*. Comparisons of performances of PPFM models led to the conclusion that the
1025 MAE error values improved and that the *RI* (“reliability”) values usually also improved as more types
1026 of input variables (chronological variables, price variables, power demand variables, forecasted
1027 weather variables, and power generation variables) were included in such PPFM models.

1028
1029 The probabilistic price forecasting models of this article, their performance, mainly in terms of
1030 MAE error and Reliability Indicator values, pragmatic calculations applied to the PDF functions
1031 associated to day-ahead probabilistic price forecasts, and the best PPFM model, can be useful for
1032 business players within electrical energy markets and other agents from the electric power industry.

1033
1034 Possible future research works related to this article would probably be aimed to improve the
1035 bandwidth calibration process, to use other probabilistic forecasting scores, and to analyze the
1036 performance of the PPFM models using a non-Gaussian KDE.

1037 **ACKNOWLEDGEMENTS**

1038
1039 The authors would like to thank the “Ministerio de Economía y Competitividad” of the Spanish
1040 Government for supporting this research under the project ENE2016-78509-C3-3-P and the ERDF
1041 funds of the European Union; and to thank the Smartwatt company (swi.smartwatt.net) for providing
1042 data and practical experience associated with the models featuring in this article.

1043 **REFERENCES**

1044
1045 [1] Weron R. Electricity price forecasting: A review of the state-of-the-art with a look into the future. Int J Forecast
1046 2014;30:1030–81. doi:10.1016/j.ijforecast.2014.08.008.

- 1048 [2] Contreras J, Espinola R, Nogales FJ, Conejo AJ. ARIMA models to predict next-day electricity prices. *IEEE Trans*
1049 *Power Syst* 2003;18:1014–20. doi:10.1109/TPWRS.2002.804943.
- 1050 [3] Cruz A, Muñoz A, Zamora JL, Espinola R. The effect of wind generation and weekday on Spanish electricity spot price
1051 forecasting. *Electr Power Syst Res* 2011;81:1924–35. doi:10.1016/j.epsr.2011.06.002.
- 1052 [4] Conejo AJ, Contreras J, Espinola R, Plazas MA. Forecasting electricity prices for a day-ahead pool-based electric
1053 energy market. *Int J Forecast* 2005;21:435–62. doi:10.1016/j.ijforecast.2004.12.005.
- 1054 [5] Bordignon S, Bunn DW, Lisi F, Nan F. Combining day-ahead forecasts for British electricity prices. *Energy Econ*
1055 2013;35:88–103. doi:10.1016/j.eneco.2011.12.001.
- 1056 [6] Karakatsani N V., Bunn DW. Forecasting electricity prices: The impact of fundamentals and time-varying coefficients.
1057 *Int J Forecast* 2008;24:764–85. doi:10.1016/j.ijforecast.2008.09.008.
- 1058 [7] Jonsson T, Pinson P, Nielsen HA, Madsen H, Nielsen TS. Forecasting Electricity Spot Prices Accounting for Wind
1059 Power Predictions. *IEEE Trans Sustain Energy* 2013;4:210–8. doi:10.1109/TSTE.2012.2212731.
- 1060 [8] Ziel F. Forecasting Electricity Spot Prices Using Lasso: On Capturing the Autoregressive Intraday Structure. *IEEE*
1061 *Trans Power Syst* 2016;31:4977–87. doi:10.1109/TPWRS.2016.2521545.
- 1062 [9] Koopman SJ, Ooms M, Carnero MA. Periodic Seasonal Reg-ARFIMA–GARCH Models for Daily Electricity Spot
1063 Prices. *J Am Stat Assoc* 2007;102:16–27. doi:10.1198/016214506000001022.
- 1064 [10] Dong Y, Wang J, Jiang H, Wu J. Short-term electricity price forecast based on the improved hybrid model. *Energy*
1065 *Convers Manag* 2011;52:2987–95. doi:10.1016/j.enconman.2011.04.020.
- 1066 [11] Knittel CR, Roberts MR. An empirical examination of restructured electricity prices. *Energy Econ* 2005;27:791–817.
1067 doi:10.1016/j.eneco.2004.11.005.
- 1068 [12] Tan Z, Zhang J, Wang J, Xu J. Day-ahead electricity price forecasting using wavelet transform combined with ARIMA
1069 and GARCH models. *Appl Energy* 2010;87:3606–10. doi:10.1016/j.apenergy.2010.05.012.
- 1070 [13] Girish GP. Spot electricity price forecasting in Indian electricity market using autoregressive-GARCH models. *Energy*
1071 *Strateg Rev* 2016;11–12:52–7. doi:10.1016/j.esr.2016.06.005.
- 1072 [14] Weron R, Misiorek A. Forecasting spot electricity prices: A comparison of parametric and semiparametric time series
1073 models. *Int J Forecast* 2008;24:744–63. doi:10.1016/j.ijforecast.2008.08.004.
- 1074 [15] Yamin H, Shahidehpour S, Li Z. Adaptive short-term electricity price forecasting using artificial neural networks in
1075 the restructured power markets. *Int J Electr Power Energy Syst* 2004;26:571–81. doi:10.1016/j.ijepes.2004.04.005.
- 1076 [16] Lin W-M, Gow H-J, Tsai M-T. Electricity price forecasting using Enhanced Probability Neural Network. *Energy*
1077 *Convers Manag* 2010;51:2707–14. doi:10.1016/j.enconman.2010.06.006.

- 1078 [17] Singhal D, Swarup KS. Electricity price forecasting using artificial neural networks. *Int J Electr Power Energy Syst*
1079 2011;33:550–5. doi:10.1016/j.ijepes.2010.12.009.
- 1080 [18] Amjady N. Day-Ahead Price Forecasting of Electricity Markets by a New Fuzzy Neural Network. *IEEE Trans Power*
1081 *Syst* 2006;21:887–96. doi:10.1109/TPWRS.2006.873409.
- 1082 [19] Li G, Liu C-C, Mattson C, Lawarree J. Day-Ahead Electricity Price Forecasting in a Grid Environment. *IEEE Trans*
1083 *Power Syst* 2007;22:266–74. doi:10.1109/TPWRS.2006.887893.
- 1084 [20] Ghasemi A, Shayeghi H, Moradzadeh M, Nooshyar M. A novel hybrid algorithm for electricity price and load
1085 forecasting in smart grids with demand-side management. *Appl Energy* 2016;177:40–59.
1086 doi:10.1016/j.apenergy.2016.05.083.
- 1087 [21] Alamaniotis M, Bargiotas D, Bourbakis NG, Tsoukalas LH. Genetic Optimal Regression of Relevance Vector
1088 Machines for Electricity Pricing Signal Forecasting in Smart Grids. *IEEE Trans Smart Grid* 2015;6:2997–3005.
1089 doi:10.1109/TSG.2015.2421900.
- 1090 [22] Cerjan M, Matijaš M, Delimar M. Dynamic Hybrid Model for Short-Term Electricity Price Forecasting. *Energies*
1091 2014;7:3304–18. doi:10.3390/en7053304.
- 1092 [23] Chen X, Dong ZY, Meng K, Xu Y, Wong KP, Ngan HW. Electricity Price Forecasting With Extreme Learning
1093 Machine and Bootstrapping. *IEEE Trans Power Syst* 2012;27:2055–62. doi:10.1109/TPWRS.2012.2190627.
- 1094 [24] Pindoriya NM, Singh SN, Singh SK. An Adaptive Wavelet Neural Network-Based Energy Price Forecasting in
1095 Electricity Markets. *IEEE Trans Power Syst* 2008;23:1423–32. doi:10.1109/TPWRS.2008.922251.
- 1096 [25] Catalao JPS, Pousinho HMI, Mendes VMF. Hybrid Wavelet-PSO-ANFIS Approach for Short-Term Electricity Prices
1097 Forecasting. *IEEE Trans Power Syst* 2011;26:137–44. doi:10.1109/TPWRS.2010.2049385.
- 1098 [26] Osório GJ, Matias JCO, Catalão JPS. Electricity prices forecasting by a hybrid evolutionary-adaptive methodology.
1099 *Energy Convers Manag* 2014;80:363–73. doi:10.1016/j.enconman.2014.01.063.
- 1100 [27] Singh N, Mohanty SR, Dev Shukla R. Short term electricity price forecast based on environmentally adapted
1101 generalized neuron. *Energy* 2017;125:127–39. doi:10.1016/j.energy.2017.02.094.
- 1102 [28] Voronin S, Partanen J. Price forecasting in the day-ahead energy market by an iterative method with separate normal
1103 price and price spike frameworks. *Energies* 2013;6:5897–920. doi:10.3390/en6115897.
- 1104 [29] Nowotarski J, Raviv E, Trück S, Weron R. An empirical comparison of alternative schemes for combining electricity
1105 spot price forecasts. *Energy Econ* 2014;46:395–412. doi:10.1016/j.eneco.2014.07.014.
- 1106 [30] Kuster C, Rezgui Y, Mourshed M. Electrical load forecasting models: A critical systematic review. *Sustain Cities Soc*
1107 2017;35:257–70. doi:10.1016/j.scs.2017.08.009.

- 1108 [31] Colak I, Sagiroglu S, Yesilbudak M. Data mining and wind power prediction: A literature review. *Renew Energy*
1109 2012;46:241–7. doi:10.1016/j.renene.2012.02.015.
- 1110 [32] Sobri S, Koochi-Kamali S, Rahim NA. Solar photovoltaic generation forecasting methods: A review. *Energy Convers*
1111 *Manag* 2018;156:459–97. doi:10.1016/j.enconman.2017.11.019.
- 1112 [33] Ahmad T, Chen H, Guo Y, Wang J. A comprehensive overview on the data driven and large scale based approaches
1113 for forecasting of building energy demand: A review. *Energy Build* 2018;165:301–20.
1114 doi:10.1016/j.enbuild.2018.01.017.
- 1115 [34] Fleten S-E, Kristoffersen TK. Short-term hydropower production planning by stochastic programming. *Comput Oper*
1116 *Res* 2008;35:2656–71. doi:10.1016/j.cor.2006.12.022.
- 1117 [35] Pinson P, Madsen H, Nielsen HA, Papaefthymiou G, Klöckl B. From probabilistic forecasts to statistical scenarios of
1118 short-term wind power production. *Wind Energy* 2009;12:51–62. doi:10.1002/we.284.
- 1119 [36] Morales JM, Conejo AJ, Perez-Ruiz J. Short-Term Trading for a Wind Power Producer. *IEEE Trans Power Syst*
1120 2010;25:554–64. doi:10.1109/TPWRS.2009.2036810.
- 1121 [37] Heredia FJ, Rider MJ, Corchero C. Optimal Bidding Strategies for Thermal and Generic Programming Units in the
1122 Day-Ahead Electricity Market. *IEEE Trans Power Syst* 2010;25:1504–18. doi:10.1109/TPWRS.2009.2038269.
- 1123 [38] Amjady N, Hemmati M. Energy price forecasting - problems and proposals for such predictions. *IEEE Power Energy*
1124 *Mag* 2006;4:20–9. doi:10.1109/MPAE.2006.1597990.
- 1125 [39] Zhao JH, Dong ZY, Xu Z, Wong KP. A Statistical Approach for Interval Forecasting of the Electricity Price. *IEEE*
1126 *Trans Power Syst* 2008;23:267–76. doi:10.1109/TPWRS.2008.919309.
- 1127 [40] Wan C, Xu Z, Wang Y, Dong ZY, Wong KP. A Hybrid Approach for Probabilistic Forecasting of Electricity Price.
1128 *IEEE Trans Smart Grid* 2014;5:463–70. doi:10.1109/TSG.2013.2274465.
- 1129 [41] Khosravi A, Nahavandi S, Creighton D. Quantifying uncertainties of neural network-based electricity price forecasts.
1130 *Appl Energy* 2013;112:120–9. doi:10.1016/j.apenergy.2013.05.075.
- 1131 [42] Wu HC, Chan SC, Tsui KM, Hou Y. A New Recursive Dynamic Factor Analysis for Point and Interval Forecast of
1132 Electricity Price. *IEEE Trans Power Syst* 2013;28:2352–65. doi:10.1109/TPWRS.2012.2232314.
- 1133 [43] Kou P, Liang D, Gao L, Lou J. Probabilistic electricity price forecasting with variational heteroscedastic Gaussian
1134 process and active learning. *Energy Convers Manag* 2015;89:298–308. doi:10.1016/j.enconman.2014.10.003.
- 1135 [44] Maciejowska K, Nowotarski J, Weron R. Probabilistic forecasting of electricity spot prices using Factor Quantile
1136 Regression Averaging. *Int J Forecast* 2016;32:957–65. doi:10.1016/j.ijforecast.2014.12.004.

- 1137 [45] Zareipour H, Janjani A, Member S, Leung H, Motamedi A, Schellenberg A. Classification of Future Electricity
1138 Market Prices. *IEEE Trans Power Syst* 2011;26:165–73. doi: 10.1109/TPWRS.2010.2052116
- 1139 [46] Huang D, Zareipour H, Rosehart WD, Amjady N. Data Mining for Electricity Price Classification and the Application
1140 to Demand-Side Management. *IEEE Trans Smart Grid* 2012;3:808–17. doi:10.1109/TSG.2011.2177870.
- 1141 [47] Tay AS, Wallis KF. Density forecasting: A survey. *A Companion to Econ Forecast* 2007:45–68.
1142 doi:10.1002/9780470996430.ch3.
- 1143 [48] Charytoniuk W, Chen MS, Kotas P, Van Olinda P. Demand forecasting in power distribution systems using
1144 nonparametric probability density estimation. *IEEE Trans Power Syst* 1999;14:1200–6. doi:10.1109/59.801873.
- 1145 [49] Hong T, Fan S. Probabilistic electric load forecasting: A tutorial review. *Int J Forecast* 2016;32:914–38.
1146 doi:10.1016/j.ijforecast.2015.11.011.
- 1147 [50] Bracale A, Caramia P, Carpinelli G, Di Fazio A, Ferruzzi G. A Bayesian Method for Short-Term Probabilistic
1148 Forecasting of Photovoltaic Generation in Smart Grid Operation and Control. *Energies* 2013;6:733–47.
1149 doi:10.3390/en6020733.
- 1150 [51] Zhang Y, Wang J. GEFCom2014 probabilistic solar power forecasting based on k-nearest neighbor and kernel density
1151 estimator. 2015 IEEE Power Energy Soc. Gen. Meet., IEEE; 2015, p. 1–5. doi:10.1109/PESGM.2015.7285696.
- 1152 [52] Jeon J, Taylor JW. Using Conditional Kernel Density Estimation for Wind Power Density Forecasting. *J Am Stat*
1153 *Assoc* 2012;107:66–79. doi:10.1080/01621459.2011.643745.
- 1154 [53] Alessandrini S, Delle Monache L, Sperati S, Nissen JN. A novel application of an analog ensemble for short-term
1155 wind power forecasting. *Renew Energy* 2015;76:768–81. doi:10.1016/j.renene.2014.11.061.
- 1156 [54] Serinaldi F. Distributional modeling and short-term forecasting of electricity prices by Generalized Additive Models
1157 for Location, Scale and Shape. *Energy Econ* 2011;33:1216–26. doi:10.1016/j.eneco.2011.05.001.
- 1158 [55] Jónsson T, Pinson P, Madsen H, Nielsen H. Predictive Densities for Day-Ahead Electricity Prices Using Time-
1159 Adaptive Quantile Regression. *Energies* 2014;7:5523–47. doi:10.3390/en7095523.
- 1160 [56] Rigby RA, Stasinopoulos DM. Generalized additive models for location, scale and shape. *J R Stat Soc Ser C (Applied*
1161 *Stat)* 2005;54:507–54. doi:10.1111/j.1467-9876.2005.00510.x.
- 1162 [57] Nadaraya EA. On estimating regression. *Theory Probab Appl* 1964;9:141–142. doi:10.1137/1109020.
- 1163 [58] Watson G. Smooth regression analysis. *Sankhyá Ser. A* 1964;26:359–372.
- 1164 [59] Juban J, Siebert N, Kariniotakis GN. Probabilistic Short-term Wind Power Forecasting for the Optimal Management
1165 of Wind Generation. 2007 IEEE Lausanne Power Tech, IEEE; 2007, p. 683–8. doi:10.1109/PCT.2007.4538398.

1166 [60] Bessa RJ, Miranda V, Botterud A, Wang J, Constantinescu EM. Time Adaptive Conditional Kernel Density Estimation
1167 for Wind Power Forecasting. *IEEE Trans Sustain Energy* 2012;3:660–9. doi:10.1109/TSSTE.2012.2200302.

1168 [61] Zhang Y, Wang J. GEFCom2014 probabilistic solar power forecasting based on k-nearest neighbor and kernel density
1169 estimator. *Proc. IEEE Power Energy Soc Gen. Meeting, Denver, CO, USA, 2015*, pp. 1–5.

1170 [62] Wand MP, Jones MC. *Kernel Smoothing*. Chapman and Hall/CRC. Boca Raton, 1995.

1171 [63] Scott DW. *Multivariate density estimation: theory, practice, and visualization*. John Wiley & Sons. New York, 1992.

1172 [64] Walpole RE, Myers RH, Myers SL, Ye K. *Probability and Statistics for Engineers and Scientists*. Prentice Hall.
1173 Boston, 2011.

1174 [65] Beta distribution. http://en.wikipedia.org/wiki/Beta_distribution (accessed December 12, 2017).

1175 [66] Gupta AK, Nadarajah S. *Handbook of Beta Distribution and Its Applications*. Marcel Dekker. New York, 2004.

1176 [67] The Iberian Energy Derivatives Exchange, OMIP. <http://www.omip.pt> (accessed December 12, 2017).

1177 [68] Market Operator of the Iberian Electricity Market, OMIE. <http://www.omie.es> (accessed December 12, 2017).

1178 [69] Red Eléctrica de España (REE). Spanish Transmission System Operator. [http://www.ree.es/es/actividades/demanda-](http://www.ree.es/es/actividades/demanda-y-produccion-en-tiempo-real)
1179 [y-produccion-en-tiempo-real](http://www.ree.es/es/actividades/demanda-y-produccion-en-tiempo-real) (accessed December 12, 2017).

1180 [70] Redes Energéticas Nacionais (REN). Portuguese Transmission System Operator.
1181 <http://www.centrodeinformacao.ren.pt/EN/Pages/CIHomePage.aspx> (accessed December 12, 2017).

1182 [71] Janjic Z, Black T, Pyle M, Ferrier B, Chuang HY, Jovic D et al. NMM Version 3 Modeling System User's Guide.
1183 http://www.dtcenter.org/wrf-nmm/users/docs/user_guide/V3/users_guide_nmm_chap1-7.pdf (accessed December
1184 12, 2017).

1185 [72] Global Forecast System (GFS). Environmental Modeling Center, National Weather Service.
1186 <http://www.emc.ncep.noaa.gov/index.php?branch=GFS> (accessed December 12, 2017).

1187